Fernando Rull-Pérez
(Editor)

Howell G. M. Edwards
David C. Smith
Peter Vandenabeele
(Co-editores)

Selected Topics in Raman Spectroscopic Applications

Geology · Bio-materials · Art

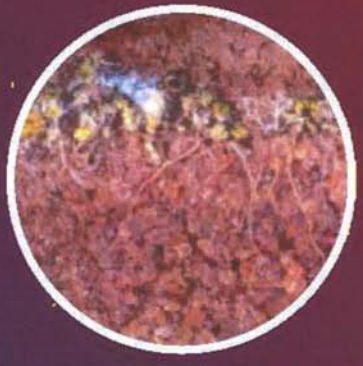

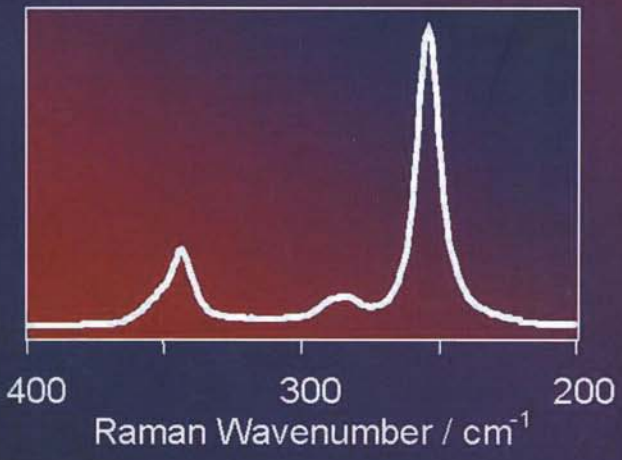

UniversidaddeValladolid

© EDITORES. Valladolid, 2007
UNIVERSIDAD DE VALLADOLID

Maquetación y Diseño de cubierta: Jesús Medina García
Antonio Sansano Caramazana

ISBN: 978-84-690-9239-2

Dep. Legal: SE-7027-2007 U.E.

Imprime: PUBLIDISA

INDEX

EDITOR.

FERNANDO RULL-PÉREZ

CO-EDITORES

HOWELL G.M. EDWARDS
DAVID C. SMITH
PETER VANDENABEELE

SELECTED TOPICS IN RAMAN SPECTROSCOPIC APLLICATIONS GEOLOGY · BIO-MATERIALS · ART

Departamento de Física de la Materia Condensada
Cristalografía y Mineralogía

Universidad de Valladolid
España

RAMAN MICROSCOPY OF CORRODED METALS IN ARCHAEOLOGY AND ART HISTORY

Michel BOUCHARD [1] and David C. SMITH [2]

[1] Getty Conservation Institute, 1200 Getty Center Drive, Suite 700, Los Angeles, CA 90049, USA; <mbouchard@getty.edu<

[2] Département d'Histoire de la Terre USM0205, and CNRS UMR7072, Muséum National d'Histoire Naturelle, 61 Rue Buffon, 75005 PARIS, France. <davsmith@mnhn.fr> and <david.smith@lgs.jussieu.fr>

Accepted 05/2004, printed 11/2007

1. INTRODUCTION

What is interesting about applying Raman Microscopy (RM) to metals in Archaeology or Art History? Three essential answers to this question can be detailed below, in addition to the specific, and sometimes unrivalled, advantages of the RM technique that have already been described in the many articles now dedicated to RM studies in what has been coined *ARCHAEORAMAN* by Smith and Edwards[1] and updated by Smith[2,3], in particular studies on:

- *pigments*[4,5,6,7,8,9,10,11];
- *biomaterials*[12,13,14,15];
- *gems*[16,17,18,19,20];
- *rocks*[21,22,23,24,25];
- *ceramics*[26,27,28,29,30,121];

- *stained glass*[31,32,33,34,35,36]; or
- *corroded metals*[37,38,39,40,41,42,35,43,44,45,46,47,48,122].

(1) One finds metals nowadays in almost all the domains that concern society. Development of the discoveries concerning metal since the Bronze and Iron Ages, as well as the infinite possible combinations of metallic elements, make this material ***indispensable***. From pipelines to skyscrapers, from vehicles to bridges, from cables to computers, not to mention coins, tools, statues and, last but not least, armaments, one finds metals almost everywhere. However, a real disease is often present: ***corrosion***. Tracking the past for archaeologists, disaster for industrialists, corrosion is a real plague that occupies many researchers (physicists, chemists, mineralogists, metalworkers etc.), and RM can help with the comprehension of this phenomenon.

(2) RM, which is a very recent technique in comparison with many others (XRD, IR, EMP...), has not yet been widely employed in the domain of metals and more precisely in the domain of corrosion. The early workers were Pardessus-Peyrol *et al.*[49], Delichere *et al.*[50], Boucherit *et al.*[51,52], Thierry *et al.*[53], Hugot le Goff *et al.*[54,55] and Bernard *et al.*[56,57,58,59,60]; these workers, mostly in the same laboratory, worked mainly on Fe, Mn and/or Zn. Nevertheless, *corroded metal constitutes an ideal material for RM*, since, although most metals do not yield Raman spectra (for reasons of high crystal symmetry, low number of atoms per unit cell, high absorption and/or high reflectivity), their corrosion products do: mainly oxides, hydroxides, carbonates, chlorides and/or sulphates, but sometimes nitrates, phosphates or silicates. Being a technique that is:

(i) non-destructive,

(ii) needs no sample preparation, not even any sampling at all in many cases,

(iii) mobile for studies really *in situ*[2,3,20],

(iv) capable of analysing a single micrometre-sized crystal and making 3D images by XY (or maybe XYZ) Raman mapping of mixtures on the micrometre scale[61,62].

Thus RM can provide details of physicochemical interrelationships of *mixed phases* within the corrosion products on a specific metallic object wherever it is: on a bridge, on an exposed statue, through glass[63] (e.g. a priceless metallic art work conserved in a jar in a Museum), at an archaeological site or even underwater (subaquatic archaeology of submerged cities or sunken ships; tanks

conserving precious artefacts awaiting restoration)[64], and all this, whatever is its surface profile on a micrometre scale (planar, curved, angular, discontinuous).

(3) One may envisage in the near future, the collaboration between a "ramanist" research team and an archaeological or artistic restoration and conservation laboratory with *the aim of preserving and preventing the alteration of archæological metals*. Indeed there is no doubt that any *ARCHAEORAMAN* project is interdisciplinary and requires collaboration between specialists in at least two, and sometimes three, of the triplet of the necessary disciplines which may be classified as (i) Archaeology, Art History, Conservation and/or Restoration; (ii) Crystallography, Mineralogy, Metallogeny and/or Geology, (iii) Chemistry, Physics and/or Spectroscopy.

Following a recent study carried out on a large corpus of corroded metallic archaeological objects[45], this chapter presents a glimpse of the advantages and the limits of the application of RM to the study of metallic corrosion products. After a brief discussion of the phenomenon of corrosion, the different results are developed and the different types of alteration products observed in practice are listed. The objective of this study is to evaluate the capacities and to demonstrate the efficiency of this analytical method recently applied to the domain of Art and Archaeology. Two previous articles by Bouchard and Smith[43,44] were dedicated to a database of standard products susceptible to be observed on archaeological material. Part of this data set were published in abstract form in Bouchard and Smith[39,41,42] and in a brief study of some archaeological artefacts in Bouchard and Smith[40]; a detailed study of corroded coins was published in Bouchard and Smith[35].

2. NOTIONS OF CORROSION

Some research on the corrosion of metals is ancient, but it was only in the late 1830's that the physicist August de La Rive proposed an electrochemical theory of this phenomenon. However, research on metal corrosion took off in the XXth century and by the end of that century, a phenomenal number of publications had appeared. The study of metal corrosion thus became almost a separate sub-discipline. For this reason this subsection will not go into all the complex problems related to the corrosion of metals.

For simplification, one can however classify corrosion in two large families: homogeneous or uniform corrosion (corresponding to the formation of a film of alteration on the surface of the metal) and heterogeneous corrosion (corresponding to localized corrosion formed by holes or craters of many μm of depth).

In the case of homogeneous corrosion, the corrosion develops at effectively the same speed at all points of the metal surface. The colour of the film of alteration (mostly green or red for copper, black/grey for silver and white for zinc) is essentially due to the combined phenomena of refraction/reflection/absorption of light at the surface of the corrosion product. The interest shown for this type of corrosion derives from the fact that this layer, whose thickness grows with time, is not always passive. Indeed, even if the layer is itself stabilized, numerous indirect parameters can permit the corrosion of the object to continue: e.g. the permeability of this outer layer to certain gases; the relative affinity of the various components of the inner alloy for these same corrosive gases; the solubility of the different components in the layer of corrosion itself; and other numerous thermodynamical factors (temperature, humidity, partial pressure of oxygen, diffusion, etc.).

In the case of heterogeneous corrosion, one speaks of (a) "pitting corrosion" or (b) "intergranular or intercrystalline corrosion". The "pitting corrosion" is localized at certain points of the metal whereas intercrystalline corrosion is localized at the joints of grains of the metal. This last type of corrosion is rather dangerous because, although the loss of metal is small, it quickly leads to a reduction of the mechanical characteristics of the metal[65].

It may be noted that, according to the environment in which the studied object has evolved, one will obtain sulphides or sulphates (for an environment rich in SO_2), carbonates (for an environment rich in CO_2), oxides (for an environment rich in O_2), chlorides (for an environment rich in chloride salts) or composite products stemming from the combined action of some of these external factors. For example, according to McCann *et al.*[38], the presence of $PbSO_4$ indicates that a Pb-bearing metallic object was in contact at a given moment in its past with H_2S and SO_2 urban pollution or with an environment of sulphate-reducing bacteria (anaerobic environment) producing H_2S. In the case of a Pb-free metallic object exposed recently in an urban environment, one can deduce that the Pb derived from petrol pollution.

Pourbaix[66] presented some other examples which allow the reconstitution of the conditions of corrosion of the studied object according to the products which are associated with it; for example if the percentage of CO_2 in the atmosphere exceeds 0.04 % (which corresponds to a rainwater of pH 5,8 with

10^{-5} moles of CO_2/litre) it forms malachite (green) as well as tenorite (black). In an atmosphere loaded with SO_2, one can, by using thermodynamical diagrams, determine the concentration of SO_2 that was necessary for the formation of the sulphide or sulphate product.

Finally, "paratacamite" (in fact *clinoatacamite*[45] and see below) $\{Cu_2Cl(OH)_3\}$, is the stable form of copper chloride in an oxygenated acid solution charged in Cl^- ions, whereas, in the absence of oxygen, the stable form is nantokite {CuCl}.

Contrary to *passive* (i.e. stabilised) corrosion, *active* (i.e. ongoing) corrosion is intrinsically "more dangerous" for the metal object. A major part of this chapter will be devoted to chlorides, a typical mode of alteration which in the case of cuprous or ferrous alloys is dramatic and irreversible. Chlorides can become hydrated and thus change in crystalline structure, and by increasing in volume soon lead to a fast destruction of the object. Iron objects, when they are chlorinated, can split completely following their lines of weakness established during their manufacture[67]. It is this type of alteration which should be neutralised first of all if one wants to limit damage, and this is the reason why the principal focus here is aimed at the identification of these products by RM. However, the main subject of this chapter remains the *identification* of the corrosion products; the reader is referred to the following works for their presentation of different neighbouring areas of problems related to the corrosion of metals[68,69,70,71,72,73,7475].

3. CORPUS OF ARCHAEOLOGICAL OBJECTS STUDIED

The considerable number of materials existing within the field of "the archaeology of metals" lead us to restrict our report to the study of some precise metals, selected mainly according to their representativity in archaeological objects. Copper, known since millennia and cited in works as ancient as the Bible or the Iliad, is the most represented metal in this study. Numerous lead and iron objects also constitute an important part of the study whereas zinc, tin, silver and gold alloy objects constitute only a small part of this work, either because of the rarity of these objects, or because of the deliberate choice of our research team. The corpus of the studied metallic objects is deliberately very varied in terms of the different types of objects and of the different cultures

which manufactured them. It partially consists of coins and medals of which the small size and the simplicity of dating make a material of choice for this type of study[35], but it also consists of numerous other archaeological objects described in detail in Table 1. Figure 1 displays some of the Pre-Columbian artefacts. These objects are also in various states of corrosion: from averagely corroded (e.g. F753-24) to totally corroded (e.g. L84-85) (Figure 2). The particular case of coins, where the metal composition is generally already known and referenced, the metal composition of the archaeological objects presented here is the one noted in *italics*: *Ag* (silver), *Al* (aluminium), *Bz* (bronze), *Cu* (copper), *Cu alloy* (copper alloy), *Fe* (iron), *Ni* (nickel), *Pb* (lead), *Sn* (tin), *Zn* (zinc). On the basis of Ponting and Segal[120]:

- *Copper* is accepted as pure for a tin and zinc concentration <1 %.
- *Bronze* is constituted in theory of 85 % of copper and 15 % of tin, but in practice one observes it with a majority of copper, more than 1 % of tin and less than 5 % of zinc. Lead is also often present and its concentration can reach 25 %. It is thus rather difficult to define a composition for bronze.
- *« Bells' Bronze »* is an alloy constituted of 78 % of copper and 22 % of tin.
- *Brass* has a composition as variable as that of bronze; one can consider that brass contains more than 5 % of zinc and less than 3 % of tin, the solvent being copper.
- *« Orichalcum »* is defined as a copper alloy with ~ 10 to 15 % of zinc.

Table 1. Corpus of the some of the studied metallic archaeological objects.

N° Ref.	Identification	Metal	Region/ Culture	Reign/Date	Results of Analysis
S2215	DENIER	*Ag*	Roman	Alexander Severus / *193-211 A.D.*	malachite, quartz, Ag_2O*
G678	1 ECU	*Ag*	France	Louis Philippe / *1843*	Ag_2O*
S894	DENIER	*Ag*	Roman	Domitian / *86 A.D.*	cuprite, Ag_2O*
S7441	DRACHMA	*Ag*	Parthes	Orodes II / *57-38 B.C.*	Ag_2O*
G471	1 FRANC	*Al*	France	*1944*	
P1	AS	*Bz*	Roman	Augustus (?) / *27 B.C.-14 A.D.*	cuprite, clinoatacamite + atacamite
S3190	SMALL BRONZE	*Bz*	Roman	Tetricus / *270-*	cuprite, malachite +

				273 A.D.	?
P2	SMALL BRONZE	*Bz*	Barbarian	*~Vth century A.D.*	tenorite, cuprite
G15	12 DENIERS	*Bz bell*	France	Louis XVI / *1792*	cuprite, malachite, clinoatacamite + atacamite
P5	medal	*Fe*	France	Commune insurrection / *1848*	goethite, lepidocrocite, phase A
G474	1 FRANC	*Ni*	France	type « Semeuse » / *1960*	
P8	MEDAL NAP. I	*Zn (?)*	France	*1840*	ZnO
G290	10 C^{tms}	*Zn*	France	*1941*	ZnO amorphous
W.C.	1 KORUNA	*Zn*	Bohemia	*1943*	ZnO amorphous
714-348	NAIL	*Cu alloy*			connellite
714-351	UNCERTAIN	*Cu alloy*			atacamite, connellite
714-569	PIN	*Cu alloy*			connellite
L84-163	TOOL FRAGMENT	*Cu alloy*			cuprite, azurite, malachite, antlerite, langite
L84-85	SCABBARD	*Cu alloy*			atacamite, clinoatacamite
F753-24	PEACOCK'S TAIL FIBULA	*Cu alloy*			amorphous zinc oxide, copper hydrochloride, cuprite, azurite
F753-26	FIBULA	*Cu alloy*			amorphous zinc oxide, copper hydrochloride, copper sulphate (langite + antlerite + ?)
547	NAIL	*Fe*			goethite, hematite
634-24	RING	*Fe*			lepidocrocite+ ?
714-1011	PLATE	*Pb*			PbO
33-90-72	GOBELET	*Ag*	Paramonga (Cerrode la Horca), Peru		Ag_2O*
78-13-132	"CEPHALOMORPHE" VASE	*Ag : 96 % Cu : 4%*	Acon, Central Coast, Peru		Ag_2O*
78-13-129	CEREMONIAL GOBLET (KERO)	*Ag : 97 % Cu : 3%*	Acon, Chimu, Peru *1000-1463 A.D.*		Ag_2O*

45-25-3	AXE	*Cu alloy*		malachite
66-141-12	FLAT AXE WITH HUMAN FACE	*Cu alloy*	Vicus, Peru 200 B.C.	clinoatacamite + atacamite, calcite
66-141-40	HAMMER HEAD	*Cu alloy*	Vicus, Peru	clinoatacamite + atacamite
66-141-52	HAMMER HEAD	*Cu alloy*		clinoatacamite + atacamite
66-141-137	MASK (MAN OR FELINE HEAD)	*Cu golden*	Mochica, Peru	clinoatacamite + atacamite
66-141-138	MASK (FELINE HEAD)	*Cu golden*	Mochica, Peru	malachite + ?
08-22-1185	MIRROR	*Pyrite*		lepidocrocite, hematite, maghemite + ?
08-22-1186	MIRROR	*Pyrite*	Ingarpirca, Ecuador	mixture : lepidocrocite, hematite, maghemite
P10/2	Waist belt or shoe	*Cu alloy*	Middle Age/ Renaissance / *XV/XVII th cent.*	malachite
P11	VASE HANDLE	*Cu alloy*	Gallic	malachite
P12	ARROWHEAD	*Fe*	Roman	lepidocrocite, hematite
110-383	PLATE SARCOPHAGE	*Pb*	Roman	plumbonacrite, hydrocerussite, cerussite (?)
L1	INGOT	*Fe*	Roman	lepidocrocite, goethite, maghemite, « $FeCl_4^-$(?) », akaganeite + goethite

*Ag_2O already existing or formed under the laser heating. The catalogues of Sear[76], Krause[77] and Gadoury[78] helped in establishing the data on the coins.

Mask (feline head) (66-141-138)

Flat axe with human face (66-141-12)

Bronze axe (45-25-3)

« Pyrite» mirrors (08-22-1185 & 08-22-1186)

Bronze hammer head (66-141-52)

Bronze vase handle (P11)

Mask (man or feline head) (66-141-137)

Bronze hammer head (66-141-40)

Figure 1. Nine Pre-Colombian objects examined (Musée de l'Homme, Paris, France)

Figure 2. Bronze scabbard (L84-85) decayed due to attack by copper chlorides.

4. RM RESULTS

The various results are grouped and presented below according to the principal metal component of the object (e.g. copper alloy objects, iron alloy objects, silver alloy objects, etc.). The various products of corrosion observed and identified on each archaeological object being detailed in Table 1, it is not necessary to re-describe them all in detail.

The major handicap that afflicts "recent" sciences such as RM is the relative deficiency of databases of reference spectra. One will see in this chapter that one of the basic principles of the identification of species by RM is the comparison of the unknown spectrum with reference spectra of standard products. Consequently, a poorly-informed database will hinder any complex identification. This why our different studies lead to the elaboration of databases of minerals susceptible to be observed on the alteration products of metals and their archaeological environment in order to strengthen the global collection of available databases[43,44,17].

It is essential to notice the difference between the benefits of a method such as RM, which allows to obtain the exact species identification of the alteration product, with those purely chemical methods such as an electron microprobe or EDS XRF with a scanning electron microscope. An EDS analysis was made on the Augustus Roman bronze coin (Ref. *P.1*, Table 1) and targeted particularly the zone rich in chlorides (Figure 3). Although the analysis was able to be achieved in a totally non-destructive way (coating was not even necessary), and although the results usefully showed the presence of trace elements such Si, Fe and Al (coming most probably from ground contamination rather than from the alloy), the identification of alteration products in this zone was limited to that of chemical elements: Cu + Cl + O without any information on their crystal structure.

Figure 3. Bronze coin of Augustus (P1) (area of the chlorides). Optical microscopy.

4.1. PRODUCTS OF ALTERATION OF COPPER ALLOY OBJECTS

4.1.1. COPPER CHLORIDES

This type of alteration constitutes active corrosion in the case of copper and is often referred to as "bronze disease"[79,80]. This type of extremely "fatal" corrosion for the archaeological object (Figure 2) has thus become a target for numerous researchers, metalworkers, chemists and mineralogists in association

with the restorators and curators. The research already made in this domain demonstrated notably the predominant role of cuprite {Cu_2O} during active corrosion by chlorides[81]. Hydrated copper chlorides {$Cu_2Cl(OH)_3$} can form in various ways, e.g. from brochantite or malachite, or from anhydrous copper chloride (i.e. nantokite {CuCl})[45,43]. In all cases "it seems necessary to consider all the active chlorides under the form of CuCl or not"[81].

4.1.1.1. Distinction between the various forms of $Cu_2Cl(OH)_3$ by RM

As indicated in Bouchard[45,43], there exists a certain 'vagueness' concerning the exact identification of the various copper chlorides.

Jambor showed in one of his works[82] the existence of another polymorph of {$Cu_2Cl(OH)_3$}: clinoatacamite. These authors demonstrated the confusion that existed between paratacamite and clinoatacamite: a real historico-mineralogical imbroglio. In addition, numerous other oxyhydroxychlorides of copper exist in Nature and are thus susceptible to be observed on the alteration products of copper: (1) pure Cu + Cl ± O ± H; (2) ditto + other anionic radicals; or (3) ditto + other metals. Thus one may quote in addition to the three polymorphs botallackite, atacamite and clinoatacamite, and also paratacamite:

(1) anthonyite {$Cu(OH,Cl_2).3H_2O$}, calumetite {$Cu(OH, Cl)_2.2H_2O$}, claringbullite {$Cu_4Cl(OH)_7.nH_2O$}, hydromelanothallite, melanothallite {Cu_2OCl_2}, nantokite {CuCl}, tolbachite{$CuCl_2$}...

(2) connellite {$Cu_{19}Cl_4SO_4(OH)_{32}.3H_2O$}...

(3) arzrunite {$Cu_4Pb_2SO_4(OH)_4Cl_6.2H_2O$}, aubertite {$CuAl(SO_4)Cl.14H_2O$}, boleite {$Ag_9Cu_{24}Pb_{26}Cl_{62}(OH)_{48}$}, chloroxiphite {$CuPb_3O_2Cl_2(OH)_2$}, cumengite {$Cu_{20}Pb_{21}Cl_{42}(OH)_{40}$}, diaboleite {$CuPb_2Cl_2(OH)_4$}, percylite {$CuPbCl(OH)_2$}, pseudoboleite {$28PbCl_2.2AgCl.24Cu(OH)_2.14H_2O$} (??), wherryite {$CuPb_4O(SO_4)(CO_3)(OH,Cl)_2$}...

Only three kinds of hydrated chlorides of copper have been identified so far on the different metallic archaeological objects here (atacamite, clinoatacamite [possibly paratacamite], and connellite[43,44]. Botallackite has not

been observed on the archaeological objects. Selected results are detailed in Figs. 2 & 3, Tables 1, 2a & 2b and Figure 3. In parallel to this work, different mineralogical samples of hydrated copper chlorides from the MNHN Mineral Collection have been analysed by RM and confirmed by XRD analysis for use as standards[45].

The actual state of the literature dealing with RM applied to the identification of atacamite and paratacamite (or clinoatacamite) is relatively poor, as a detailed comparison of the Raman spectra of the various polymorphs is non-existent[45,43,83].

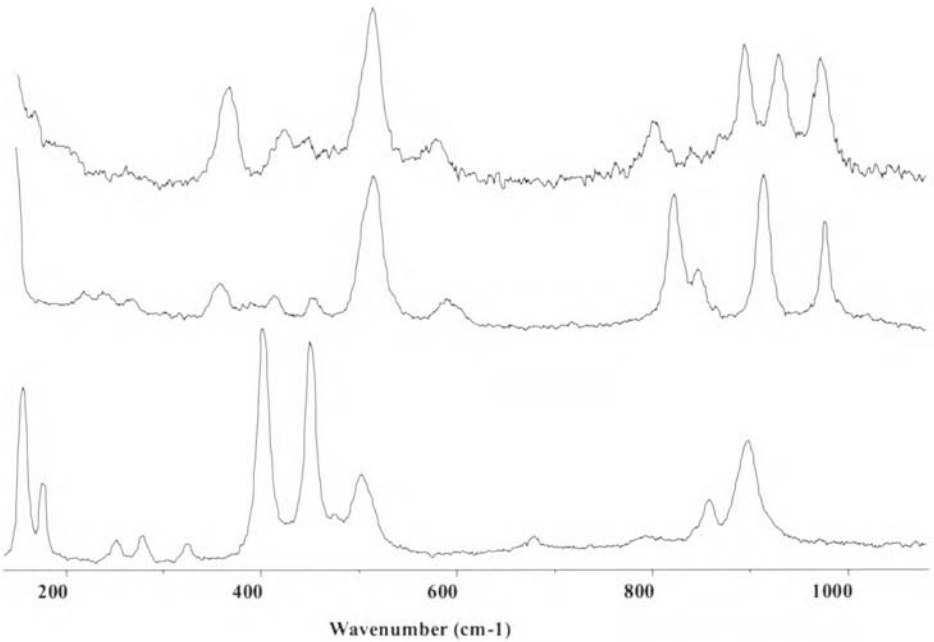

Figure 4. Raman spectra of an archaeological clinoatacamite (ref. G15) (BRCU05LE) (top); an atacamite (CTAN5LE) (middle); and a standard botallackite (FNCU6LE) (bottom). The code numbers in brackets in this and following figures are names of the relevant spectrum's computer file.

Table 2a. The different Raman bands attributed to atacamite and to clinoatacamite, in cm^{-1}.

Ref.	mineral species	Raman bands

B	atacamite		360			513			821	846		911		974
G	atacamite					516			827	850		918		980
Pt	clinoatacamite**	...	364	420	450	511	590	**804**	(820)	(842)	896	911	**930**	975
Pt	atacamite**	...	358	412					820	842				
Pt	botallackite	...	**324**	**401**		503	(678)			**857**	897			

B: Bell *et al.*[5] (1997). G: Guineau[84] . Pt: present work. ** attributed name;
In this and all following tables the symbolisation indicates: underlining: stronger peaks; brackets: weaker peaks; bold type: characteristic bands unique to one of these species.

Fig. 4 and Table 2a reveal many spectral distinctions between botackallite and clinoatacamite, but clinoatacamite shows many spectral overlaps with atacamite.

Fig. 5 and Table 2b shows that the distinct bands corresponding to hydroxyl group (O-H) stretching in the 3400 cm^{-1} region would, alone, be sufficient to differentiate all three polymorphs

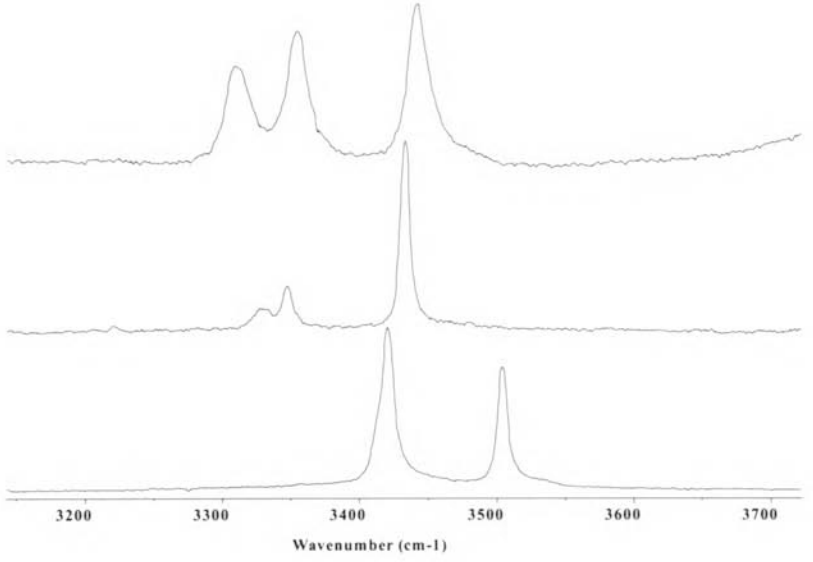

Figure 5. Raman spectra of an archaeological clinoatacamite (ref. G15) (BRCU05LE) (top); an atacamite (CTAN5LE) (middle); and a standard botallackite (FNCU6LE) (bottom).

Table 2b. Position of the different Raman bands at the very high region of wavenumbers for the spectra type A (atacamite), type B (clinoatacamite) and botallackite, in cm^{-1}.

Pt	type. B	clinoatacamite **	**3310** wide			**3355** wide	**3442** wide	
Pt	type. A	atacamite**		**3327**	**3347**		**3433**	
Pt		botallackite				**3420**		**3504**

4.1.2. COPPER HYDROXY-CARBONATES

4.1.2.1. Malachite

Excepting kolwezite $\{(Cu,Co)_2(CO_3)(OH)_2\}$, of black to beige colour, all the other copper carbonates are blue, green or close to these two colours[85]. The most representative and the most common species of this type of alteration of copper is malachite $\{Cu_2CO_3(OH)_2\}$; of characteristic green colour, this hydroxy-carbonate, which in fact corresponds to the classic terminology of "patina" on the objects of copper alloy, forms in an ambient concentration of CO_2 and in a high humidity. Malachite can form for example in an aqueous environment and in alkaline *pH* according to the reaction: $2Cu^{2+} + 2OH^- + CO_3^{2-} \leftrightarrow Cu_2CO_3(OH)_2$ or from brochantite according to the following reaction:

$$Cu_4SO_4(OH)_6 + 2HCO_3^- \rightarrow Cu_2CO_3(OH)_2 + SO_4^{2-} + 2H_2O \qquad [2]$$

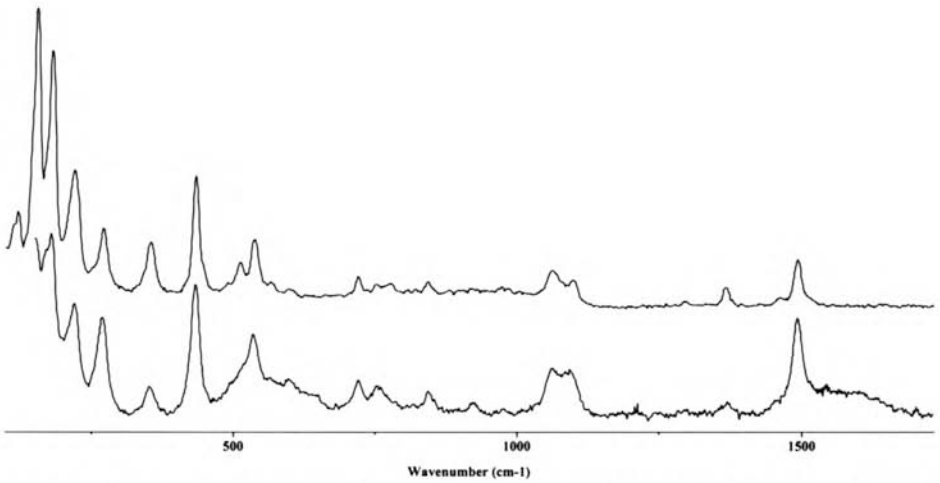

Figure 6. Raman spectra of an archaeological malachite (ref. G15) (bottom) (BRCU04) and a standard malachite (from the collection of the MNHN) (top) (BNCU37); (the band at 512 cm^{-1} probably comes from a contamination by linarite $\{CuPbSO_4(OH)_2\}$[45]).

Malachite has been observed and detected by RM on many archaeological objects based on copper (Table 1; Fig. 6,), but also on a silver coin (Table 1; Fig. 7). This sort of alteration, cf. azurite, is harmful for the conservation of the object[66], but it can also hinder observation of the object itself.

Most of the characteristic Raman bands of malachite are globally correctly reproduced by different authors (154, 180, 219, 270, 355, 434, 538, 721, 753, 1067, 1100, 1367, 1462, 1493 cm^{-1})[5,84,17]. Bands at 3308 and 3378 cm^{-1} corresponding to OH bonding in malachite, as well as the band at 1462 cm^{-1}, do not seem to have been listed by the authors mentioned above.

Figure 7. Denier of Alexander Severus (S2215) with the green outgrowth corresponding to malachite. Optical microscopy.

4.1.2.2. Azurite

Another very well-known hydroxy-carbonate had been observed: azurite $\{Cu_3(CO_3)_2(OH)_2\}$ which forms at a higher concentration of CO_2 and/or in a weaker relative humidity than malachite. The disparity of colour between these two carbonates results from an optical effect deriving from differences in bonding between both crystalline structures[85].

The spectra of the archaeological azurite seem to be absolutely identical with the spectra of standard azurite[5,38,45] and very different from standard malachite (Figs. 6 & 7). There is no major difference from spectra already recorded for this mineral species and one can distinguish easily the bands attributed to the carbonate group at ~ 1100-1600 cm^{-1}. The principal Raman bands of azurite are at 39, 177, 249, 283, 334, 402, 543, 764, 839, 938, 1098, 1424, 1458, 1578, 3423 cm^{-1}.

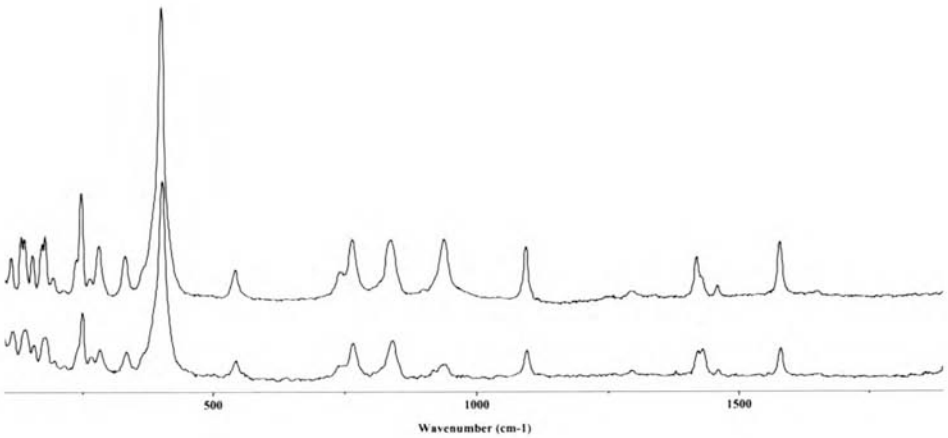

Figure 8. Raman spectra of an archaeological azurite (ref. L84-163) (top) (CGBL05) and a standard azurite (bottom) (BNCU05).

One can also mention other carbonated alteration products of copper susceptible to be observed on archaeological objects but not yet recorded: chalconatronite $\{Na_2Cu(CO_3)_2.3H_2O\}$ or georgeite $\{Cu_5(CO_3)_3(OH)_4.6H_2O\}$.

The interest of RM in the detection of this type of alteration product is mostly related to the differentiation between this kind of passive product and more "dangerous" active products, which, in contrast to malachite, have to be immediately neutralised (e.g. copper or iron chlorides).

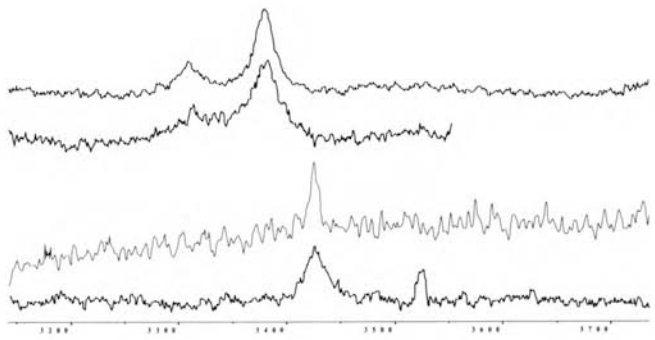

Figure 9. Raman spectra of the region of high wavenumbers (OH bands); from top to bottom: a standard malachite (BNCU37); an archaeological malachite (ref. G15) (BNCU05); a standard azurite (FGCU02) and an archaeological azurite (ref. L84-163) (CGBL04).

4.1.3. COPPER SULPHIDES AND HYDROXY-SULPHATES

4.1.3.1. Langite and antlerite

Less known than the previously-mentioned alteration products, this kind of corrosion is nevertheless relatively common on archaeological objects of copper alloy. RM particularly allowed to identify and to differentiate langite $\{Cu_4SO_4(OH)_6.2H_2O\}$ from antlerite $\{Cu_3SO_4(OH)_4\}$ (Plate 5). Previous studies [43,45] have attributed the Raman spectrum of langite to that of brochantite, this was partly due to the existence of a mixture within the mineral standard sample of brochantite and a correlation of the acquired Raman spectrum with incorrect data [87]. Previously langite was wrongly considered as being identical to brochantite; today langite is considered as a dimorph of wroewolfeite $\{CuSO_4(OH)_6.2H_2O\}$[86]. The Raman spectrum presented below has been successfully correlated with the spectrum of langite presented by Frost (2003). Due to their chemical resemblance, numerous Raman bands of langite and antlerite are similar in wavenumber (Fig. 6) and the Raman bands specific to each species are hard to distinguish despite the crystallographic difference (a monoclinic structure for langite instead of orthorhombic for antlerite). The specific bands are differentiated in Table 3. The stretching bands of the OH groups in langite and in antlerite are easily distinguished. One can also compare in this table the various bands attributed to the internal vibrations of the SO_4^{2-} group (free form): $v_1(SO_4^{2-}) = 980$ cm^{-1} (observed here at 989 and 975 cm^{-1} for respectively antlerite and langite); $v_2(SO_4^{2-}) = [422 \& 456]$ cm^{-1} (observed here at [416 & 444] cm^{-1} and [429 & 449] cm^{-1} for respectively antlerite and langite); $v_3(SO_4^{2-}) = 611 \& 617$ cm^{-1} (observed here at [604 & 630] and [611 & 621] cm^{-1} for respectively antlerite and langite); and $v_4(SO_4^{2-}) = 1098$cm^{-1} (observed here at 1098 cm^{-1} for langite).

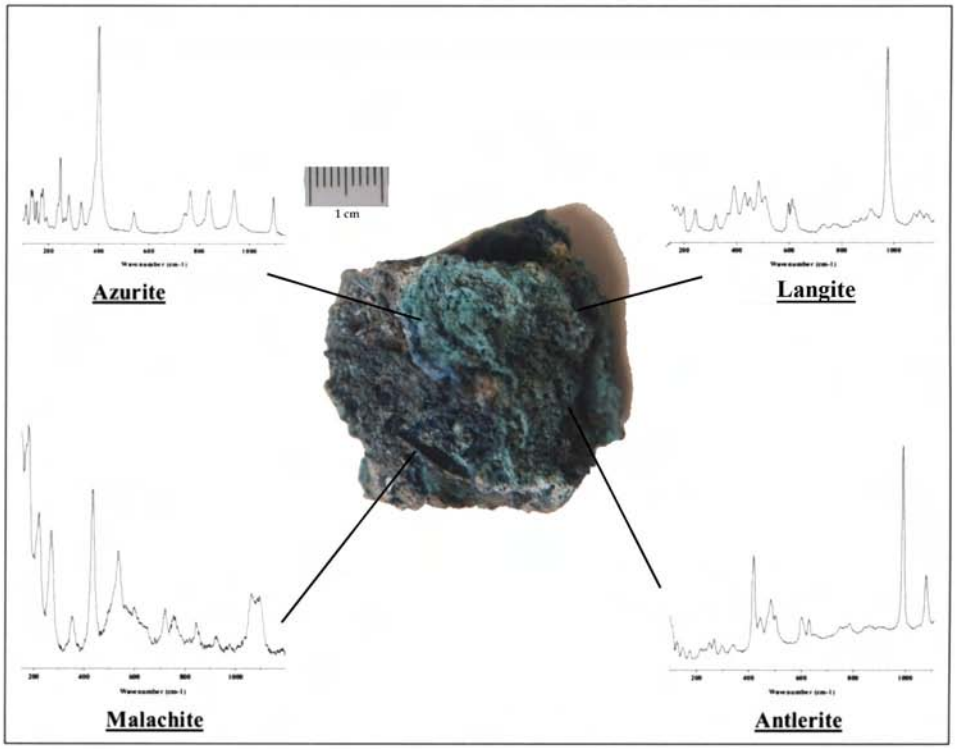

Figure 10. Archaeological bronze object (L84-163) presented with the Raman spectra of the different mineralogical phases that have been observed.

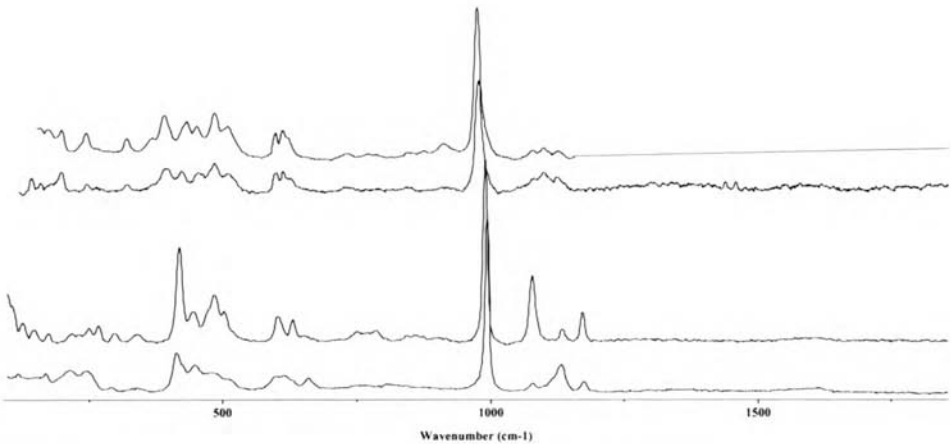

Figure 11. Raman spectra of copper hydroxy-sulphates, from top to bottom: a standard langite (ref. 65-44) (BSCU06); an archaeological langite (ref. L.84-137) (DGCU17); a standard antlerite (ref. 101-197) (BOCU08); and an archaeological antlerite (ref. L.84-163) (CRCU08).

Table 3. Raman bands specific to antlerite and langite in cm^{-1}

antlerite	langite		antlerite	langite
125				599
148			604	611
172	171		630	621
	198		750	(730)
217			(770)	
(230)	(233)		785	(785)
249	243		(911)	
265			989	975
298			1078	1078
340	320			1098
	366		1133	1125
	390		1171	
416				1565
	429			3370
444	449		3488	3400
470				3562
483	483		3580	3585
501	506			

The situation is much more distinct in the OH band region (Fig. 12).

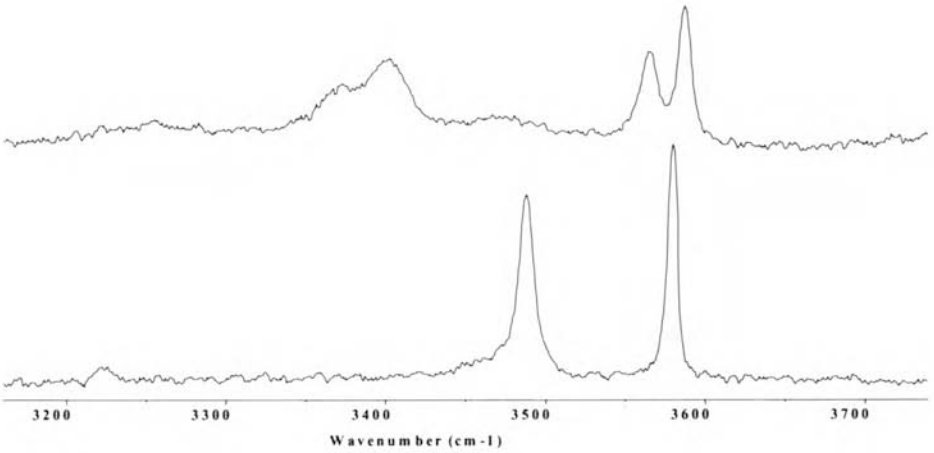

Figure 12. Raman spectra of the OH band region: standard langite (ref. 65-44) (top) (BSCU06); standard antlerite (ref. 101-197) (bottom) (BOCU08).

There also exist many other alteration products of sulphides or sulphates, more or less hydrated, that can be found in Nature under the mineral name of: bonattite $\{CuSO_4.3H_2O\}$, caledonite $\{Cu_2Pb_5(SO_4)_3(CO_3)(OH)_6\}$, chalcocyanite $\{CuSO_4\}$, chenite $\{CuPb_4(SO_4)_2(OH)_6\}$, digenite $\{Cu_9S_5\}$, djurleite $\{Cu_{31}S_{16}\}$, dolerophanite $\{Cu_2OSO_4\}$, elyite $\{CuPb_4SO_4(OH)_8\}$, nakauriite $\{Cu_8(SO_4)_4(CO_3)(OH)_6.48H_2O\}$, posnjakite $\{Cu_4SO_4(OH)_6.H_2O\}$, and the dimorphs langite and wroewolfeite $\{Cu_4SO_4(OH)_6{\cdot}2H_2O\}$. They might be encountered in corroded archaeological metals.

As in the case of the carbonates of copper described above, sulphates of copper do not seem to be of any danger for the objects. The diagram of stability of these products, presented by Pourbaix[66], indicates the domain of passivity of this type of alteration product in ambient conservation conditions.

4.1.4. COPPER OXIDES

4.1.4.1. Cuprite and tenorite

Copper oxides are exclusively represented in the analysed samples by cuprite {Cu_2O} (or cuprous oxide) of red to red/orange colour and by tenorite {CuO} (or cupric oxide); the latter species being recognizable with difficulty by RM because of its dark and blackish colour.

Cuprite forms on copper alloy objects following the electrochemical reaction:

$$Cu \rightarrow Cu^{+} + e^{-} \text{ (oxidation)} \qquad [3]$$

Potential of oxidation : $E_1 = 0.521 + 0.0591.\log(Cu^{+})$

$$\tfrac{1}{2} O_2 + 2e^{-} \rightarrow O^{2-} \text{ (reduction)} \qquad [4]$$

Thus:

$$2Cu + \tfrac{1}{2} O_2 \rightarrow Cu_2O$$

Without entering into all the details related to the different modes of corrosion and the polarities (cathodes/anodes) of the layers of cuprite, Fig. 13 presents a simplified scheme of the various electrochemical reactions on the surface of the metal, as well as on the internal and external interfaces of cuprous oxides layer, and the mechanisms of migrations of the e^{-} and Cu^{+} ions in the cuprite layer. It is also necessary to note the importance of the role of cuprite[81] in the phenomenon of active pitting corrosion essentially because of its semi-conducting proprieties.

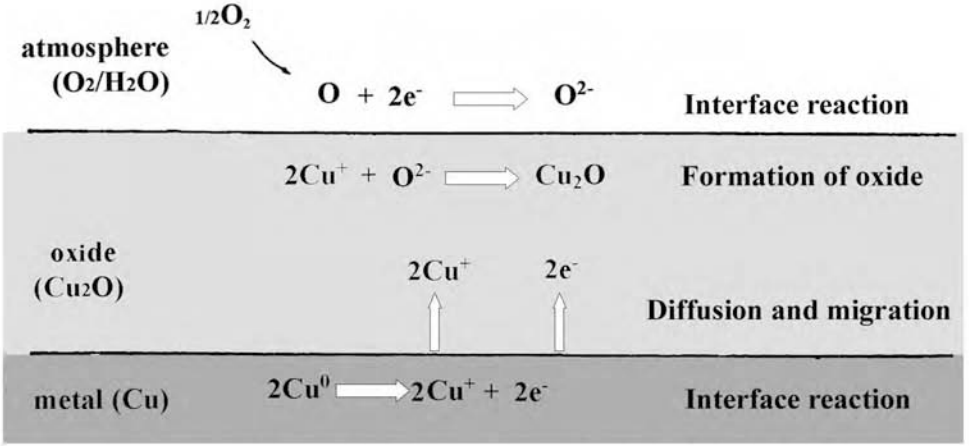

Figure 13. Theoretical scheme of the model of reaction during the formation of a copper oxide layer in an aerated environment[88,45].

4.1.4.2. Cuprite by RM

Cuprite is a rather common alteration product of copper. It was thus predictable to obtain a number of Raman spectra of this mineral on the studied metallic objects (Table 1; Figure 14). Some of these spectra were chosen to clarify certain doubtful zones. A certain heterogeneity in the spectra retained our attention. It seems that the fluctuations are related to three phenomena.

Figure 14. Denier of Domitian (S894) with the red outgrowth corresponding to cuprite.

(1) It was observed that cuprite, generally denoted {Cu_2O}, often has in fact a composition {$Cu_{2-x}O$}, where "x" can be as high as to 2.10^{-3} at high temperatures[74,89]; hence, this could possibly explain some variations observed in the Raman spectra.

(2) Cuprite shows several more bands than the simple group theory foresees in the first order[90,91]. However, one can also have multiphoton processes (harmonic, or additive or subtractive combinations), or phonon activation (forbidden in the first order in a perfect crystal) by the presence of imperfections: interstices, structure vacancies, impurities, local mechanical tensions, etc.

(3) Cuprite can, in very particular conditions, oxidize into CuO (tenorite)[74]: $2Cu_2O + O_2 \rightarrow 4CuO$

Tenorite can thus be obtained in the particular case of our study either from a phenomenon of natural oxidation, or from an oxidation due to the heating by the laser. The presence of tenorite is confirmed by certain Raman bands specific to CuO and already listed in the literature[92,38]. Thus questions reside in the distinction of

- "pure" tenorite {CuO};
- "pure" cuprite {Cu_2O};
- vacancy structures from the {$Cu_{2-x}O$) variant;
- mixtures of phases.

Table 4 lists different works made by RM on tenorite and on cuprite. The spectra are either theoretical spectra, calculated from a crystallo-physical study of the mineral, or experimental spectra. These are compared with a Raman spectrum obtained on the alteration products of the Barbarian bronze coin (ref. P2), and presenting characteristic bands of both cuprite and tenorite (Fig. 15).

Table 4. Raman bands of cuprite and tenorite in cm^{-1}

Cu_2O	Symmetric mode (R)		Γ_9	Γ_8	$\Gamma_{10,TO}$		A_g	B_g			Γ_4		B_g	$\Gamma_{10,TO}$		
	Symmetric mode (K)		Γ_{25} Γ_{2u}	Γ'_{12} E_u	Γ_{15} Γ_{1u}		A_{1g} A_{2g}	Γ'_2 A_{2u}			Γ'_{25} Γ_{2g}			Γ_{15} Γ_{1u}		
	Mc	*Exp.*					220	309		433		523	629			
	Re	*Exp.*	58, 100	110	148, 168	197	219	300		419	485	516	597	625	642	
	Ku	*Theo.*	105	110	146							515	611			
Pt	Pt	*Exp.*	~ 90	106	147	198	218	283-295	325-338	414	500	520		620	weak	
Cu_2O	Xu	*Exp.*						288-295	330-342					621-628		
	Mc	*Exp.*						297	345							

Exp.: experimental. *Theo.:* theoretical.
Pt: present work; Mc[38]; Re[93]; Ku[94]; Xu[92] (wavenumbers depending on the crystal size).

Whereas some bands are identical ± 1 cm^{-1}, others differ from those of cuprite by 5-15 cm^{-1}; these differences may well be due to vacancy cuprite. The rest of the acquired spectra are related to cuprite and are very similar with the data exposed by the authors mentioned above. The main characteristic bands which allow the distinction of tenorite from cuprite in the Barbarian coin are 283-295 and 330-342 cm^{-1} which correspond to tenorite only, whereas the bands at 106, 147, 198 and 218 cm^{-1} characterize cuprite.

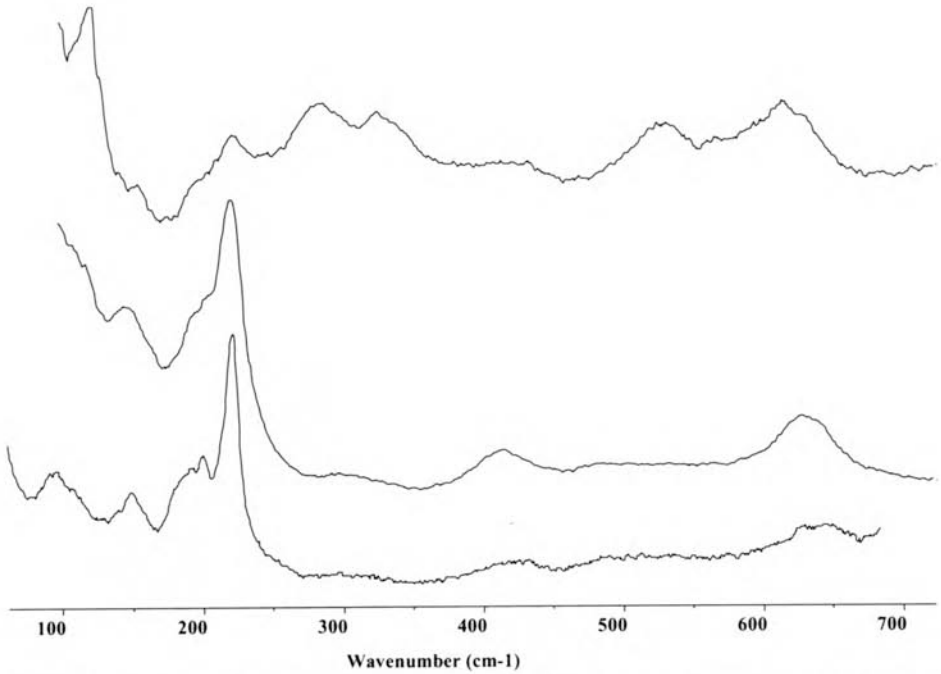

Figure 15. Raman spectra of "pure" standard cuprite (bottom) (BSCU12), an archaeological cuprite (middle) (ref. P1) (BHMO09) and a cuprite/tenorite mixture presented in Table 4 (top) (BICU03).

The role and the implication of cuprite in the phenomena of active corrosion by chlorides[81] contradicts the previously-deduced passive role of this type of alteration product of copper[95]. Cuprite is a product of corrosion susceptible to mask another phenomenon, such as chloride corrosion, which leaves the restorers and curators with the difficult task of estimating the potential danger of such a product according to their conditions of conservation.

There are also other oxides or hydroxides that one might find in the alteration products of copper and of which one knows the equivalents in nature under the mineral names: paramelaconite $\{Cu_4O_3\}$ and spertiniite $\{Cu(OH)_2\}$[95]. Numerous organic alteration products of copper such as the oxalate moolooite $\{CuC_2O_4.nH_2O\}$, diverse acetates $\{Cu(CH_3COO)_2\}$ or formates... are not dealt with here (unpub. data).

4.1.5. OTHER PRODUCTS OF COPPER

Silicate alteration products of copper have not been developed in this report. This type of product might exist on objects issue from archaeological soil. One can quote some minerals existing in the natural state and susceptible to be observed on archaeological metals: apachite $\{Cu_9Si_{10}O_{29}.11H_2O\}$, gilalite $\{Cu_5Si_6O_{17}.7H_2O\}$, luddenite $\{Cu_2Pb_2Si_5O_{14}.14H_2O\}$, plancheite $\{Cu_8[Si_4O_{11}](OH)_4.H_2O\}$, or shattuckite $\{Cu_5(SiO_3)_4(OH)_2\}$.

4.2. PRODUCTS OF ALTERATIONS OF ZINC

4.2.1. CASE OF ZINC OXIDE

RM analyses of "pure" zinc archaeological objects concerned only a few objects, mainly because of the recent industrial use of this metal (from 1740 in England). Zinc is known since Antiquity for its use in alloys. One finds it notably, according to Dioscoride (I^{st} century A.D.), in antique Greece for the cementation of copper, but it seems to be quoted for the first time under its current name only by Paracelse, at the beginning of the XVI^{th} century, in his Treatise on Metallurgica.

Analyses were made on a medal of unknown metal dated 1840 and struck with Napoleon I^{st}'s effigy (ref. P8) and on two zinc coins of the XX^{th} century : a French coin of 10 Ctms (ref. G290) and a coin of 1 Kr from Bohemia (ref. W.C.). Visual observation of the medal of Napoleon I and of its characteristic alteration of white micro-crystals allowed us to emit the hypothesis of a zinc composition of the object. It had been thought logical, in the last century or two, that this simple observation was sufficient to consider the change described as being the creation of some zinc oxide. However Scott[96] related the following anecdote: lead was found amongst the white-coloured alteration products during analyses made on the "patina" of a bronze statue; it would have been justifiable

then to suppose that this lead resulted naturally from the alteration of the bronze alloy; the metallographic analyses of the statue showed, on the contrary, that there is no trace of lead in the alloy and it was thus demonstrated that this layer of alteration formed only by deposit, a consequence of the industrial pollution in the particularly intense lead pollution in England under the Victorian reign.

RM analysis of the corrosion products of the medal ref. P8 yielded a spectrum showing a strong band at 430 cm^{-1} in addition to bands at 202, 327, 379, 570(wide) cm^{-1}, these being typical of well-crystallized zinc oxide (ZnO) (Table 5; Figs. 10,11). Both the other studied coins (refs. G290 and W.C.) present a layer of grey-white corrosion similar to that observed on the medal. Their RM analyses also yielded the spectrum of zinc oxide. These identifications are confirmed by the reference spectra of zinc oxide stemming from our own database[45,43,44] but also by the spectra published by Xu *et al.*[92]. One can note in some archaeological spectra, as well as in that acquired on the standard of ZnO, the presence of Raman bands at 1070 and 1150 cm^{-1}. Damen[97] and Phillips[98] considered that these two bands correspond to a "multiphoton" phenomenon. This hypothesis is debatable and it is necessary not to neglect the position of one of the main bands of hydrozincite situated in 1062 cm^{-1}. In this latter case, there could be a little contamination by hydrozincite, the enthalpy of formation of which is very low (DHf = 828.25 Kcal / mole); hence it is very susceptible to be formed at the same time as the ZnO oxide (DHf = 83.76 Kcal / mole) (or even preferentially)[99].

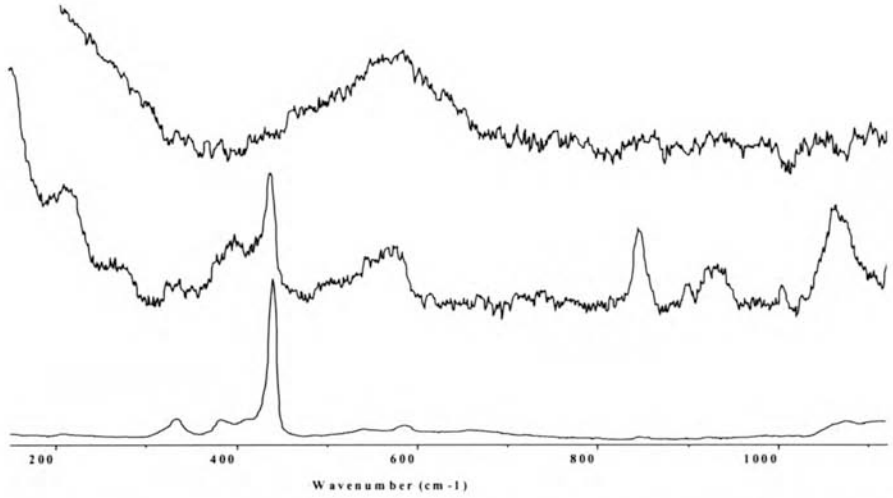

Figure 16. Raman spectra of different zinc oxides: amorphous state (bronze fibula 753-24) (FDCU11) (top); averagely crystallised (medal P8) (DQUN08) (middle); and standard ZnO (CTZN03) (bottom).

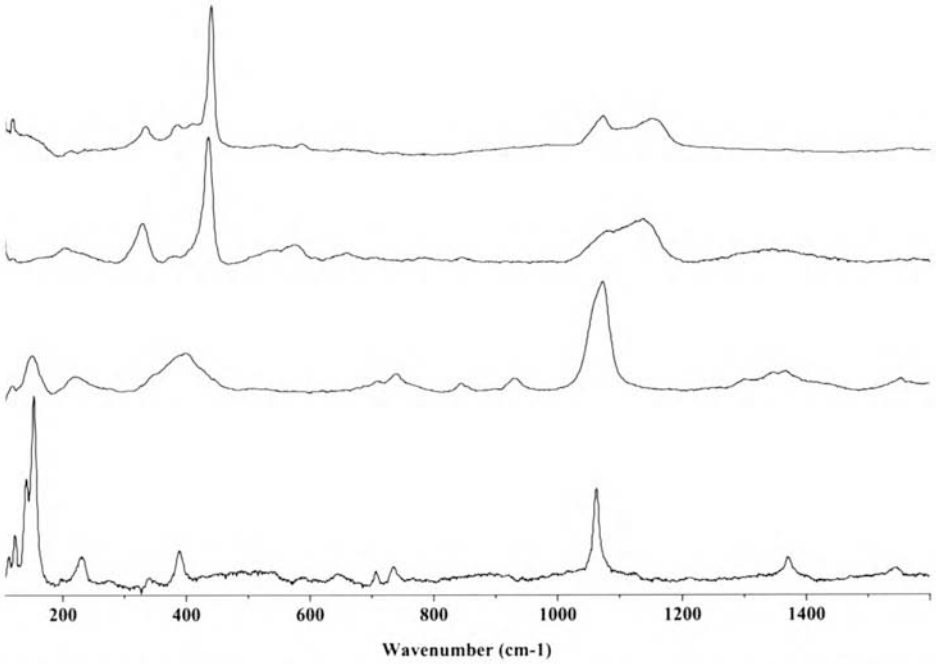

Figure 17. Raman spectra from bottom to top : standard hydrozincite (CSZN03); an archaeological hydrozincite observed on the 1 Kr (ref. W.C.) (EAUN14); zinc oxide obtained on the same coin (EAUN12); and standard zinc oxide (CAZN09).

Table 5. Raman Bands of zinc oxide on different artefacts and a standard reference, in cm^{-1}

Provenance	Raman Bands										
Fibula F753-24 and 753-26							~577				
Medal P8	202	327	(379)		430	sh	~570		~1068		
ZnO standard	(205)	332	380	(410)	437		582	(658)	1062	1076	1150
10 ctms G290	202	330	377		436	sh	570	650	1050		1150
1 Kr W.C.	202	327	379		430	sh	572	658			

sh: shoulder at ~540 cm^{-1} often observed in the spectra of poorly-crystallized zinc oxides.

Another type of spectrum, recorded on the Bohemian coin (Table 6 and Fig. 17), corresponds very well to the spectrum of hydrozincite[45].

Table 6. Raman Bands of hydrozincite on different artefacts and a standard reference, in cm^{-1}

Hydrozincite N° 100-385	81	121	139	152	230	389	704	735		1061			1371	1544
1 Kr W.C.		123		150	224	390	705	737	*930*	1065	*1297*	*1345*	1370	1548

Remark: the bands at *930, 1297 & 1345* cm^{-1} (also observed on other spectra of non-certified hydrozincite) have not been related to any other known species: hydrozincite ?; another phase ?; parasites?

The Raman spectrum at high wavenumbers of the standard sample of ZnO (Fig. 18) reveals the very wide band around 3400 cm^{-1} typical of the H_2O molecule which is presumably adsorbed on this sample. However the bands just below 3500 cm^{-1} and 3600 cm^{-1} (indeed the most intense part) resemble a structurally-bonded OH group[100].

Figure 18. Raman spectrum at high wavenumbers: standard sample of ZnO (CAZN09).

4.3. PRODUCTS OF ALTERATION OF SILVER-BASED METALS

4.3.1. CASE OF THE OXIDE OF SILVER (AG_2O)

Analysis of all the studied silver objects (including a silver Pre-Columbian statue: figure 19), as well as of a sample of chlorargyrite {AgCl}, yielded a Raman spectrum which presents a reproducible wide band at 230-240 cm^{-1}. The intensity of this band increases significantly with the duration of exposure under the laser (Fig 20). This observation permits the presumption that a new product forms by heating. Current knowledge as regards to the Raman spectrum of silver oxide[101] leads us to believe that the product formed is most probably cubic {Ag_2O}. Furthermore, Pascal[102] confirmed that a thin film of silver oxide can be obtained by heating silver in the presence of oxygen at a temperature ≥ 200°C. Other bands are observed in the zone 500-640 cm^{-1} in certain spectra of the same silver objects. At the current stage of our knowledge, the band formed at 235 cm^{-1} is considered as indicative of the presence of silver in the analysed object; regrettably, this example also shows that in certain rare cases, RM can turn out to be destructive in the sense that it leads to the formation of a new product even if this takes place on the scale of a micrometre.

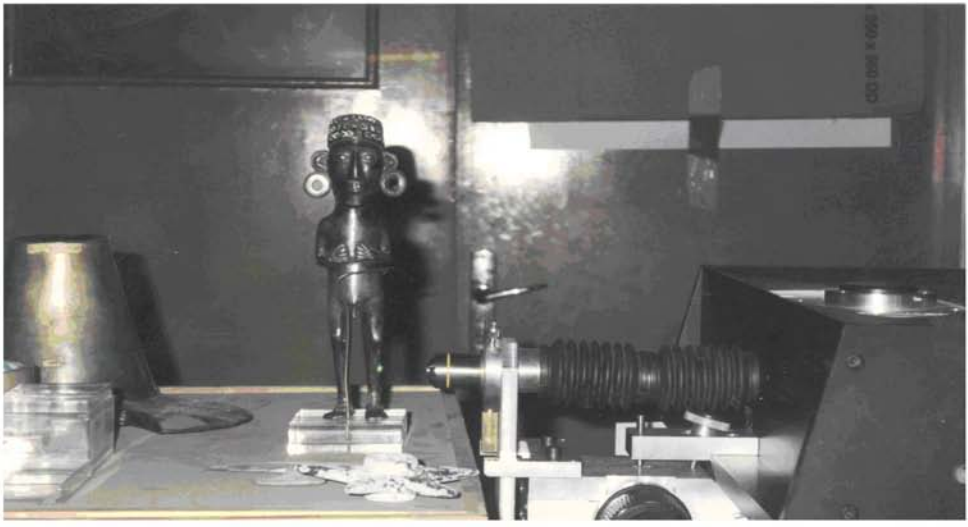

Figure 19. In situ analyses of the corrosion of a silver Pre-Columbian statue in the reserve, "Département Amérique" of the Musée de l'Homme, Paris, France. Note the green spot of the laser beam on the statue's left knee, and the horizontal microscope.

Silver oxide $\{Ag_2O\}$ happens to have the same space group as cuprite $\{Cu_2O\}$: $O_h^4 = Pn3m$[101]. According to these authors, the band observed in $\{Ag_2O\}$ at 230 cm^{-1} could be correlated to the G_2' symmetric mode band (theoretically calculated at 224.2 cm^{-1}). Bands observed at 500-600 cm^{-1} in $\{Ag_2O\}$ could also be attributed to the mode of symmetry G_{25}' calculated at 504 cm^{-1} and considered as a very wide band.

Another hypothesis, related to the first, envisages the formation of Ag particles under the heating of the laser, which provokes then an increase of the SERS effect of the pre-existent or created $\{Ag_2O\}$[45,43].

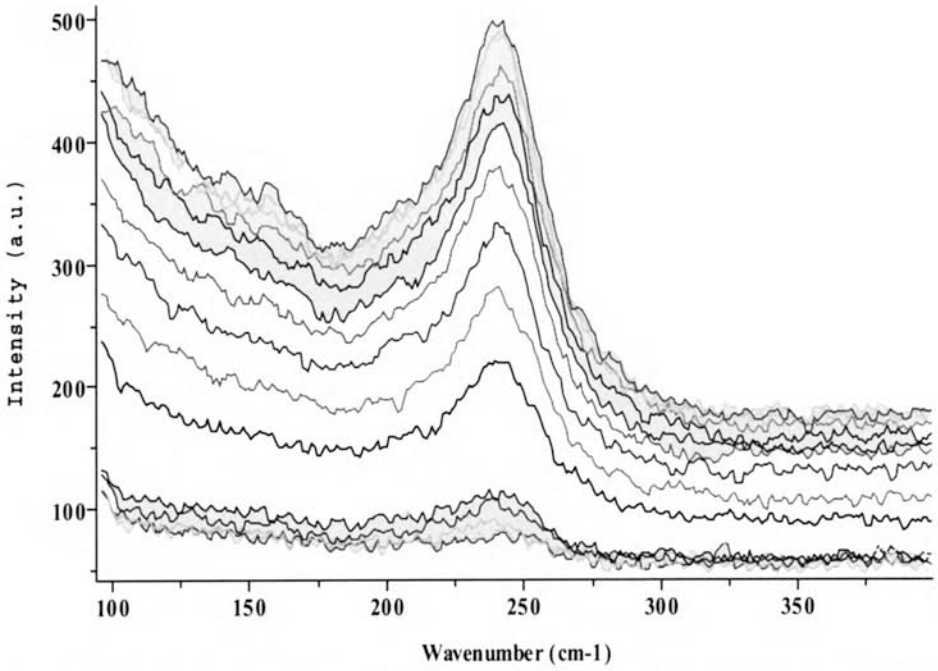

Figure 20. The band at ~235 cm^{-1} increasing as a function of the time of exposure under the laser beam (series of spectra, each of constant acquisition time) acquired on the same point showing the Raman intensity always increasing; total time here = 240 s)

4.3.2. CASE OF PREFERENTIAL OXIDATION

This phenomenon, which has already been met with in the case of bronze alloys, was again encountered in the silver alloys. It was observed on two Roman silver coins, the denier of Alexander Severus (ref. 2215) and the denier of Domitian (ref. 894); these present respectively a green and a red corrosion. If the best known and the most common alteration for silver objects is the *sulphide* of silver that one can observes on silverware, there can form on silver alloys some copper alteration products deriving from the copper in the composition of the silver alloy. In fact there exist many alloys where the concentration of solute (in this case: Cu) can exceed that of the solvent (in this case: Ag), notably in objects of a very weak grade of silver or in the case of "filled" coins.

This phenomenon can be mainly explained by the higher affinity of oxygen for copper than silver. One can thus observe in these cases the migration of the copper ions from the alloy to the outside of the object. Raman analysis of the alteration products on the two deniers cited above revealed a spectrum of malachite (green) in the case of the denier of Alexander Severus (Figure 7) and a spectrum of cuprite (red/orange) in the case of the denier of Domitian (Figure 14).

4.4. PRODUCTS OF ALTERATION OF LEAD-BASED METALS

The analysis of the corrosion products on lead objects (cf. those on iron objects) presents some difficulties related to the intimate coexistence of multiple mineral phases in very small volumes. This leads inevitably to Raman spectra superposing the characteristic bands of several kinds of minerals present under the beam of the laser. This phenomenon is exemplified by the analyses made on a lead sheet from a Roman sarcophagus (ref.110-383), which was archived in the Collections of Mineralogy of the National Museum of Natural History in 1910 because of the characteristic alteration that it has on its surface (Fig 21). This was identified as being of "cotunnite" {$PbCl_2$} at that time, but no trace of

cotunnite, identifiable by its reference Raman spectrum[45], was discovered on the analysed sample.

Figure 21. The lead sheet of a sarcophagus: Gallery of Mineralogy of the MNHN (110-383).

4.4.1. LEAD CARBONATES AND HYDROXY-CARBONATES

The study of the lead sheet of the sarcophagus allowed us to recognize the characteristic bands of plumbonacrite $\{Pb_{10}(CO_3)_6O(OH)_6\}$ as previously described by Brooker *et al.*[103]. Two other phases were also identified, although less well represented (some overlapping bands); these are hydrocerussite $\{Pb_3(CO_3)_2(OH)_2\}$ (DHf = 457.5 Kcal / mole) and cerussite $\{PbCO_3\}$ (DHf = 167.1 Kcal / mole)[99].

It is somewhat complicated to attribute the various Raman bands obtained on lead carbonates and hydroxy-carbonates since band positions common to plumbonacrite, hydrocerussite and cerussite are numerous. The possible attributions in Table 7 are based on bands observed and published by Brooker *et al.*[103] and Bouchard[45]. A small majority of the bands are specific only to

plumbonacrite. Furthermore there are specific bands to cerussite only (89, 148, 173 and 227 cm^{-1}) and there is band specific to hydrocerussite only (45 cm^{-1}). Several other bands may derive from two or three species.

Table 7. Raman Bands in cm^{-1} of plumbonacrite (P), hydrocerussite (H) and cerussite (C) observed on the lead sheet of the sarcophagus

Spectrum	**Raman Bands**													
attribution	*H*	*C, P*	*C*	*C, H, P*	*C*	*C, H, P*	*C, H, P*		*C*	*C*		*C*	*P*	*P*
DMPB06													275	306
DIPB05	**45**	58			**89**	104	121	132		166	201	**(227)**	280	307
DIPB06		56	65	71		101	117		**148**	**173**				

Spectrum	further Raman Bands									
attribution	*P*	*P*	*P*	*P*	*C,H, P*	*H, P*	*C,H, P*	*C, P*	*P*	*P*
DMPB06	401	421	460	489	681	867	1053	1380	3544	3556

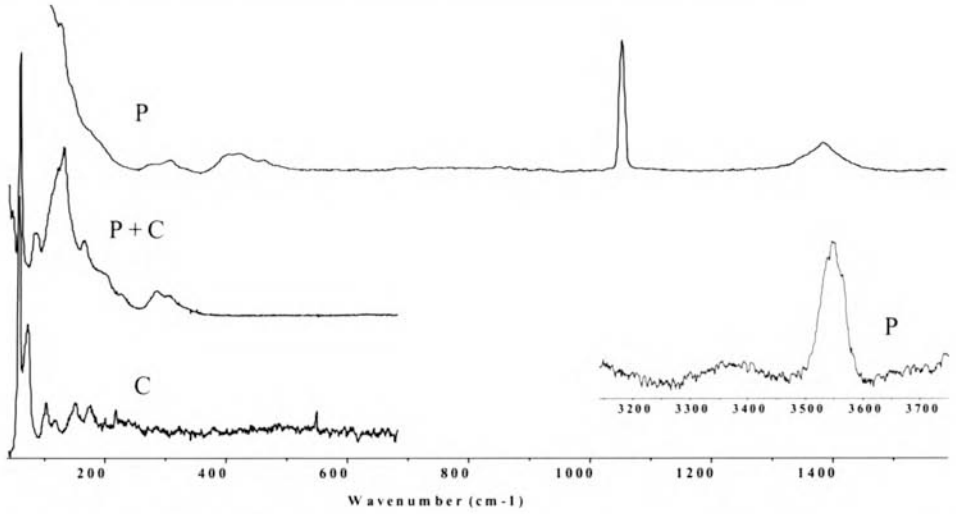

Figure 22. Raman spectra of the different mineralogical phases observed on the Roman lead sheet: plumbonacrite (top: P) (DMPB06); plumbonacrite and cerussite (middle: P+C) (DIPB05); traces of cerussite (bottom: C) (DIPB06). Inset: high region of wavenumbers; bands at 3544 and 3546 cm^{-1} characteristic of plumbonacrite (DMPB06).

4.4.2. LEAD OXIDES

Another lead sheet (ref. 714-1011), uncertainty undated (probably of Roman or Middle Age period) presented diverse alteration products. Two polymorphs of {PbO} were distinguished: litharge and massicot. Bell *et al.*[5] attributed two different Raman spectra for each of these polymorphs; massicot with Raman bands at 143, 289 and 385 cm^{-1} and litharge with bands at 145, 285 and 336 cm^{-1}. One determining factor for the differentiation of these polymorphs is the shift between the band 144 cm^{-1} of massicot with the band at 147 cm^{-1} of litharge (our wavenumbers: see Fig. 23).The bands at 285 and 289 cm^{-1} respectively attributed to litharge and massicot are wider and weaker such that they cannot be considered alone as a determining factor for the distinction of these polymorphs. On the other hand, the band at 340 cm^{-1} seems, according to Bell *et al.*[5] to be attributable only to litharge whereas the band at 385 cm^{-1} is attributable only to massicot. By taking into account these various attributions and the work of Burgio *et al.*[10], one can draw the following conclusions:

- one spectrum obtained on this sample seems to be of litharge alone as it presents Raman bands at 147 and 341 cm^{-1} (CHPB05) (Fig. 23).

- another spectrum presents bands at 144, 289, 341, 385 (weak) cm^{-1} (CHPB06) and thus seems to be a *mixture* of litharge (band at 341 cm^{-1}) and massicot (band at 385 cm^{-1}).

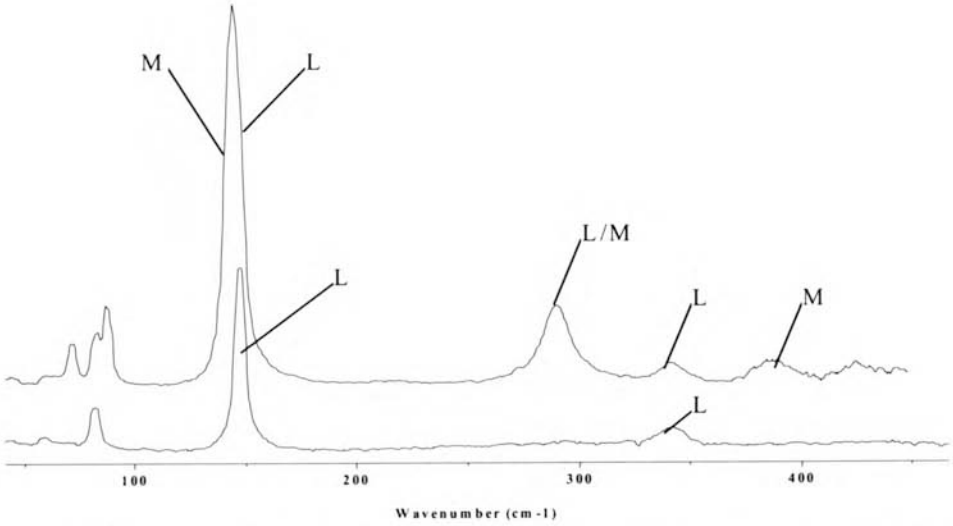

Figure 23. Raman spectra of the different phases observed and identified on the lead sheet 7141011: a mixture of litharge (L) and massicot (M) (top) (CHPB06); litharge alone (bottom) (CHPB05).

4.5. PRODUCTS OF ALTERATION OF IRON-BASED METALS

It is principally oxides and chlorides of iron that are dealt with here. There are of course numerous other types of iron alteration susceptible to be studied by RM in future studies (carbonates, sulphates, phosphates, etc.).

As in the case of alteration products of lead, in the field of iron alteration products a complexity exists in the precise identification of the various mineral phases. One can observe in the same Raman spectrum a remarkable mixture of different corrosion products produced from iron: for example lepidocrocite {γ-FeOOH}, maghemite {γ-Fe_2O_3} and hematite {α-Fe_2O_3} where the analysis took place on a surface of the order of only a few micrometre squares. Maghemite, whose structure was discussed for a long time[104,105], is now considered as metastable; it can form by dehydration of lepidocrocite or by

oxidation of magnetite (such that it is possible to find a residue of a reactant coexisting with the product). Presumably it can also form metastably directly from metallic iron.

The complex conditions of obtaining some of these iron oxy-hydroxides have been discussed by numerous researchers. Taylor[106,107] and Taylor and Schwertmann[108] showed for example how the oxidation of a solution of Fe^{2+} chloride, under certain experimental conditions, resulted in the simultaneous formation of lepidocrocite, goethite and *ferrihydrite* (unfortunately four different compositions for this species have been found in the literature: $\{Fe^{3+}_5O_7(OH).H_2O\}$, $\{Fe^{3+}_5O_7(OH).4H_2O\}$, $\{Fe^{3+}_{4\text{-}5}(OH,O)_{12}\}$ & $\{Fe^{3+}_4O_6{\cdot}H_2O\}$ such that it is most hazardous at present to try to identify ferrihydrite by RM).

An increase of temperature, or the modification of certain concentrations in Fe^{2+} or Fe^{3+}, favoured the preferential formation of maghemite. These authors also demonstrated that lepidocrocite and maghemite formed simultaneously during the oxidation of Fe^{2+} solution at *pH* 7. Boucherit *et al.*[51] noted the great difficulty of obtaining magnetite or "pure" maghemite with their stoichiometric structure, since the composition $\{Fe_{3-x}O_4\}$ (with $x < 0.33$) is much more common. Furthermore, the Raman spectra of magnetite as well as of maghemite are not yet admitted by all the researchers in the domain[109]. The situation is similar to, but not as bad as, that of oxides and oxyhydroxides of manganese where several species give the same Raman spectrum which is certainly that of a species created under the laser (cf. Ag_2O) (Smith, unpub. data; Bouchard, unpub. data).

The most common phases of iron alteration, goethite, lepidocrocite and/or hematite, were observed and identified on a ring (ref. 634-24), the medal (ref. P5), the ingot (ref. L1), both pre-Columbian pyrite mirrors (refs. 08-22-1185 and 08-22-1186), the arrowhead (ref. P12), as well as an antique nail (ref. 547). These three kinds of alteration of iron are now well-known and identified by RM[110,109]. Goethite can be specifically characterized by a Raman band at low wavenumbers (92 cm^{-1})[111,34]. This type of iron alteration product does not present at first sight any danger for objects[66]. Nevertheless, in certain conditions of concentration, temperature and *pH*, they can favour the formation of more dangerous products such as iron chlorides.

The presence of iron sulphates on iron archaeological objects was also examined. These alteration products are indeed as dangerous for iron as chlorides, the misdeeds of SO_2 being particularly impressive on iron. According to Scully[74], one can observe for example the formation of 15 to 40 "molecules" of products of degradation of iron for only one molecule of SO_2. This can be explained by a process of SO_2 chain reactions which form permanent cycles of corrosion. One can quote as follows in summary form the cycle of regeneration

of acid, where it is sulphuric acid which is regenerated cyclically, until the total degradation of the initial phase which was iron metal:

$$Fe + H_2SO_4 \rightarrow FeSO_4 \rightarrow Fe_2(SO_4)_3 \rightarrow FeOOH + H_2SO_4 \quad [7]$$

It turned out (fortunately) that none of the objects analysed, presented traces of sulphate or iron sulphides. The detection of sulphates should nevertheless remain a priority in the preventive conservation of altered iron objects, especially since sulphates are easily recognizable by RM thanks to the considerable Raman intensity of the group SO_4^{2-}. The alteration products of iron are, as those of copper, very numerous in nature. The following list mentions some of the other single metal species that might be identified on archaeological iron alteration products: amarantite $\{Fe_2O.(SO_4)_2.7H_2O\}$, beraunite $\{Fe^{2+}Fe_5^{3+}(PO_4)_4(OH)_5.6H_2O\}$, diadochite $\{Fe_2(PO_4)(SO_4)(OH).5H_2O\}$, greigite $\{Fe_3S_4\}$, ferrous hydroxide $\{Fe(OH)_2\}$, ferric hydroxide $\{Fe(OH)_3\}$, lausenite $\{Fe_2(SO_4)_3.6H_2O\}$, marcasite $\{FeS_2\}$, melanterite $\{FeSO_4.7H_2O\}$, pyrrhotite $\{Fe_xS_y\}$ (4C, 5C, 6C, 7C or 11C), rozenite $\{FeSO_4.4H_2O\}$, vivianite $\{Fe_3(PO_4)_2.8H_2O\}$ and the dimorphs phosphosiderite and strengite $\{Fe(PO_4).2H_2O\}$.

4.5.1. EFFECT OF THE LASER ON IRON OXY-HYDROXIDES

Iron alteration products need a relatively important incident laser power due to their relatively high absorption. However, if the power employed is too strong, it can provoke local damage in the order of the μm) which could be misleading in the case of a overhasty interpretation of a spectrum. It is indeed the very weak stability of some of these minerals that makes their analysis extremely delicate. De Faria *et al.*[109] explain how the dehydratation of lepidocrocite produces maghemite. This phenomenon can even happen with a weak laser power, depending upon grain size; furthermore, this transformation is not obviously observable by eyes.

Goethite can also easily dehydrate and produce hematite under the influence of the heating of the laser, but this transformation is accompanied by a flagrant alteration of colour (from yellow to red) which can be effectively

instantaneous. One may bear in mind that goethite remains the most stable kind of all simple iron hydroxides in a hydrous atmosphere.

Another example is that of magnetite, a dark and opaque alteration product, strongly absorbing and thus rather fragile. Its study by RM requires a very weak laser power and a relatively long time of acquisition. If the intensity of the laser is too important, hematite can form via a transformation of magnetite into maghemite (reaction 8)[109].

$$Fe_3O_4 \xrightarrow{200°C} \gamma\text{-}Fe_2O_3 \xrightarrow{400°C} \alpha\text{-}Fe_2O_3$$

Well-crystallised hematite is now well identified and defined by RM. Numerous works have been carried out on this mineral species, whether on corrosion products of iron objects, or on pigments. Most of authors agree to admit as characteristic of hematite 7 bands (224, 245, 291, 299, 411, 498, 611 cm^{-1}) as well as the much wider band at ~1310-1330 cm^{-1} which corresponds to an "two magnon" effect. The band at 411 cm^{-1} of well-crystallised pure hematite is particularly sensitive to variations caused by chemical replacement (e.g.: Al, Mn) or by the temperature of the sample.

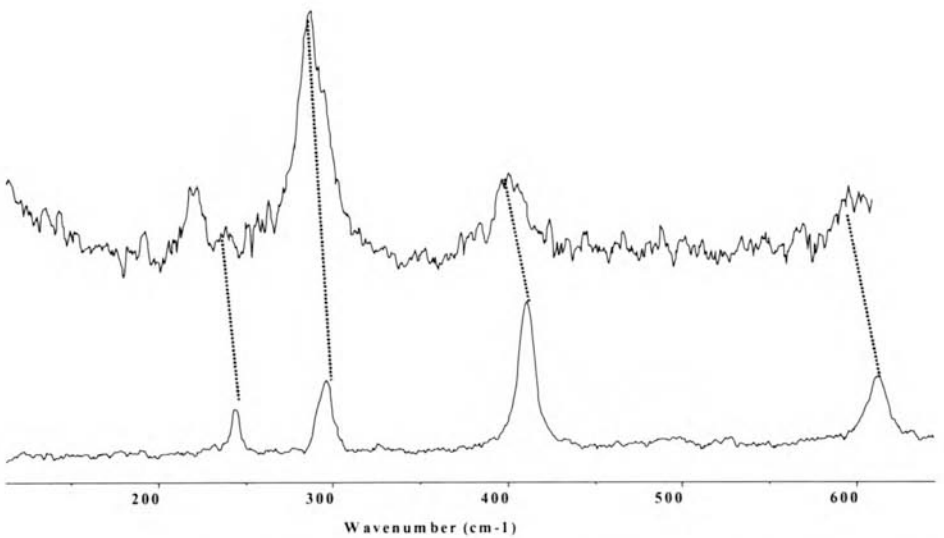

Figure 24. Raman spectra of a heated archaeological hematite (nail P547) (top) (BYFE16) and of a standard hematite (bottom)[45]

It seems that the heating undergone by the crystals of hematite may become permanent effect. Indeed, the Raman spectrum of "warmed" hematite

stayed the same during later analyses led on the same micro-crystal (analysis with weak intensity laser and several minutes after the heating). In this case, the heating caused an irreversible disordering of the structure in contrast to reversible geometric expansion shown by many other minerals.

De Faria *et al.*[109] observed that under laser heating the spectrum of hematite shows its bands enlarged and decreased in wavelength. During certain analyses we had the occasion to verify this phenomenon (Fig. 24). When some crystals were subjected to a sudden involuntary heating (a too high laser power) Raman spectra obtained in these cases (Pt in Table 8) correspond perfectly with De Faria's observations (F in Table 8). The wavenumber at 400 cm^{-1} also happens to occur in a pigment described as "disordered goethite"[34] since most of the spectrum resembled goethite more than hematite; this was deduced to represent an intermediate stage in-between goethite to hematite as they both have the same topology of the oxygen network. Other workers have used terms like hydroxyhematite or protohematite but their characterisation is not yet very clear.

Table 8. Raman Bands of standard and heated haematite.

	Ref.	Raman bands							
Standard Hematite	Pt	υ (cm^{-1})		244	293	297	410	(494)	610
		FWHM (cm^{-1})		*6.5*	*8*	*8*	*9*		*14.5*
	F	υ (cm^{-1})	226	245	292	299	411	497	612
		FWHM (cm^{-1})	*4.8*	*6.0*	*7.1*	*8.5*	*11.6*	*21.2*	*14.4*
Heated Hematite	Pt	υ (cm^{-1})	220	(*)	284	292	400		599
		FWHM (cm^{-1})	*11*		*14*	*15*	*25*		*30*
	F	υ (cm^{-1})	219	236	283	295	396	492	596
		FWHM (cm^{-1})	*10.2*	*22.0*	*20.0*	*17.3*	*29.3*	*51.9*	*39.9*

FWHM: Full Width at Half Maximum intensity

(*) corresponds to the presence a very weak band

4.5.2. THE PARTICULAR CASE OF THE IRON INGOT OF ST. MARIE DE LA MER

Iron ingots were retrieved from the cargo of the Roman wreck discovered by the D.R.A.S.S.M. (Department of Subaquatic and Submarine Archaeological Research) at Sainte-Marie-de-la-Mer (France). Three ingots were deposed with the association *Arc'Antique* in order to elaborate a suitable scheme of treatment and conservation. The research programs made in collaboration between *Arc'Antique* and the Archaeological Museum of Val d'Oise (France) led to comparative studies on the dechlorination of these ingots by a hydrogen plasma technique *and/or* by an alkaline sulphite bath treatment. These two methods aim to eliminate the chlorides present in the iron metal and archaeological objects, knowing that these alterations of iron are extremely dangerous for the object since they are able to mineralise the object completely and in a short time (in favourable atmospheric conditions).

The ingot used during these analyses was able to be sacrificed because of the absence of a historical inscription on its surface. The ingots are relatively well-preserved and this can be notably explained by their central and protected position within the cargo load of concretioned ingots (figures 25, 26). The ingot used for the study by RM is an iron bar of around 30 cm long and 5 cm width. It was decided to saw the ingot into two parts to facilitate its the manipulation and transport.

Numerous factors including (1) a layer of rather porous corrosion, (2) the long conservation in a maritime environment, and (3) the presence of acid droplets at its surface, implied the presence of chlorides within the ingot. An EDS analysis confirmed the presence of chlorine within the corrosion layers. The rapid reaction of polished sections in an ambient atmosphere (white effervescence) revealed the presence of iron chlorides $\{FeCl_2\}$[112,113].

25a

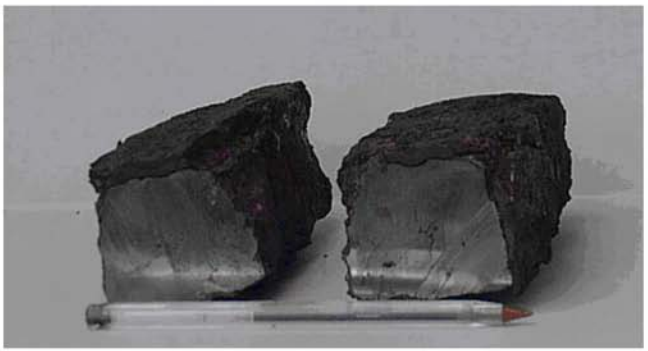

25b

Figure 25. Iron ingots and a section through one of them; the corroded part measures less than 0.7 cm deep.

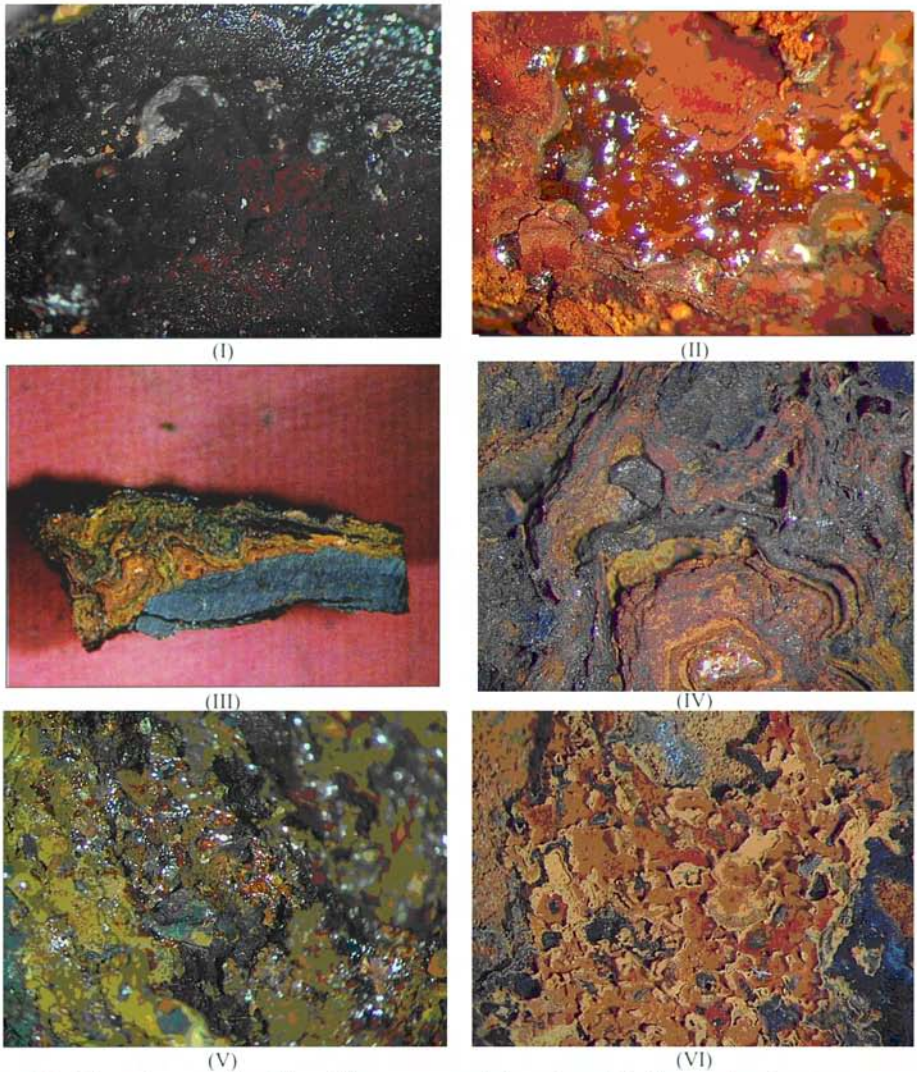

Figure 26. Microphotographs of the different types of alteration of the Roman iron ingot
(I): type (e);
(II): type (c), magnification 11,5×;
(III): general section, magnification 2,5×;
(IV): detail of III, magnification 8,3×;
(V): type (d), magnification 7,2×;
(VI): type (a), magnification 5,5×;

4.5.2.1. Analyses by RM of the corrosion layers

A coupled study between RM and hydrogen plasma (at Guiry-en-Vexin) was made to examine the effects of the dechlorination on the ingot. Raman analysis was made on the surface at 4 localised points, as well as at 3 stages of the dechlorination: t_0 (no dechlorination), t_1 (6 hours in the plasma dechlorination), t_2 (12.25 hours in the plasma dechlorination). Certain fragments of the ingot were also analysed *in section* by RM (Figs 25, 26). Five kinds of spectra have been identified so far and are listed in Table 9:

Table 9. Raman bands of the different types of iron oxy-hydroxides observed on the Roman ingot, in cm^{-1}.

Kinds	Raman Bands																		
type (a)					250					380									
type (b)	91						298				389			479			550		
type (c)		140		218	251			310	348	379					529			649	
type (d)	91	140	205				298	310			389	415	480				550		722	920
type (e)	91	140		217	250	299	310		349		388						540		

type (a) Characterises pure lepidocrocite (γ-FeOOH)

type (b) Characterises pure goethite (α-FeOOH)

type (c) Mixture 1 of lepidocrocite + maghemite (γ-Fe_2O_3) + " $FeCl_4^-$(?) "

type (d) Mixture 2 of akaganeite + goethite + " $FeCl_4^-$(?) "

type (e) Mixture 3 of lepidocrocite + goethite + " $FeCl_4^-$(?) " + maghemite

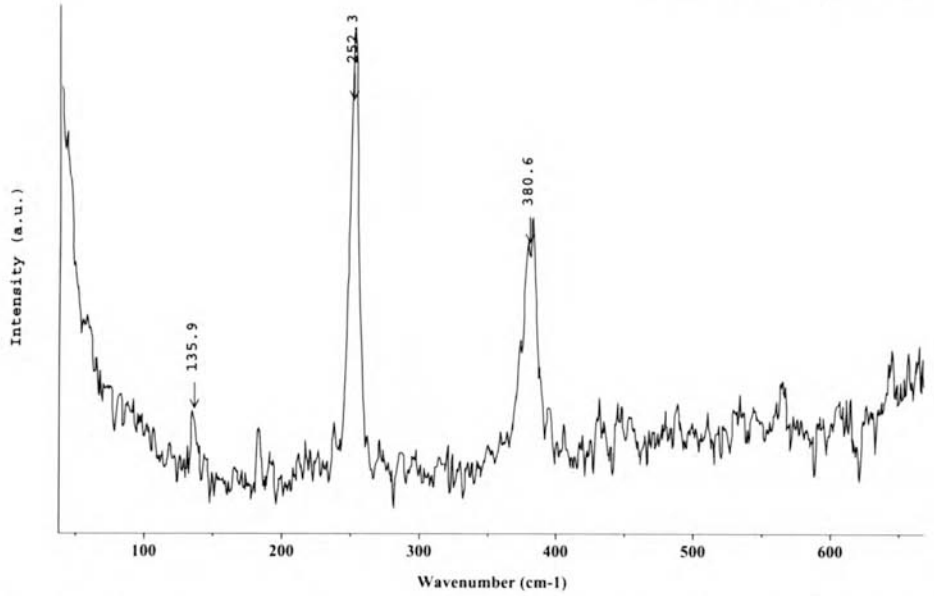

Figure 27. Raman spectrum of type (a) of oxy-hydroxide observed on the Roman ingot: (DZGU08)

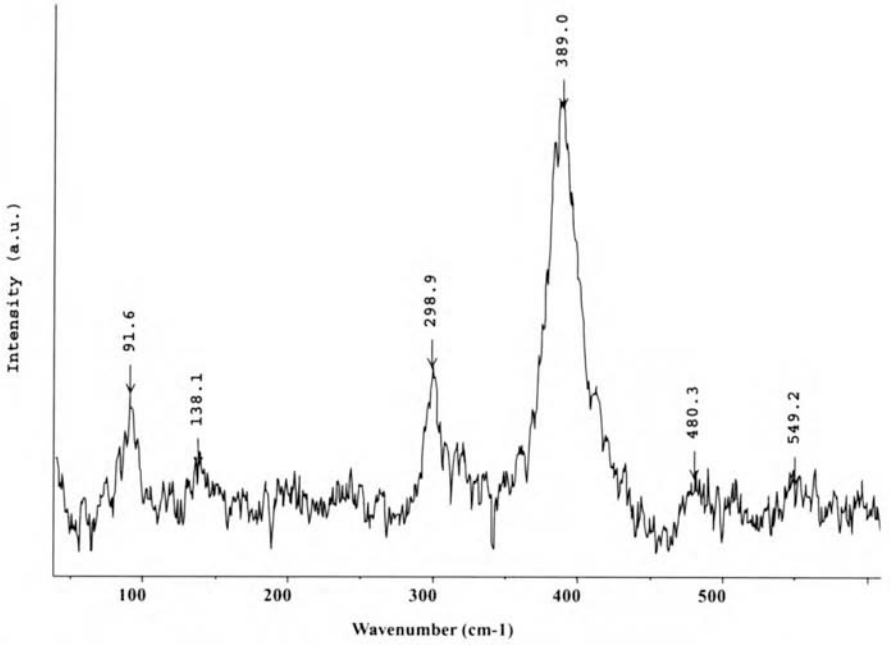

Figure 28. Raman spectrum of type (b) of oxy-hydroxide observed on the Roman ingot: (ECGU04)

Type (a) (or lepidocrocite) presents two of the four specific bands[45] of this mineral: 250, 380 cm^{-1}. Type (b) corresponds to pure goethite which has bands at 91, 298, 389, 479, 550 cm^{-1} [109,111,45].

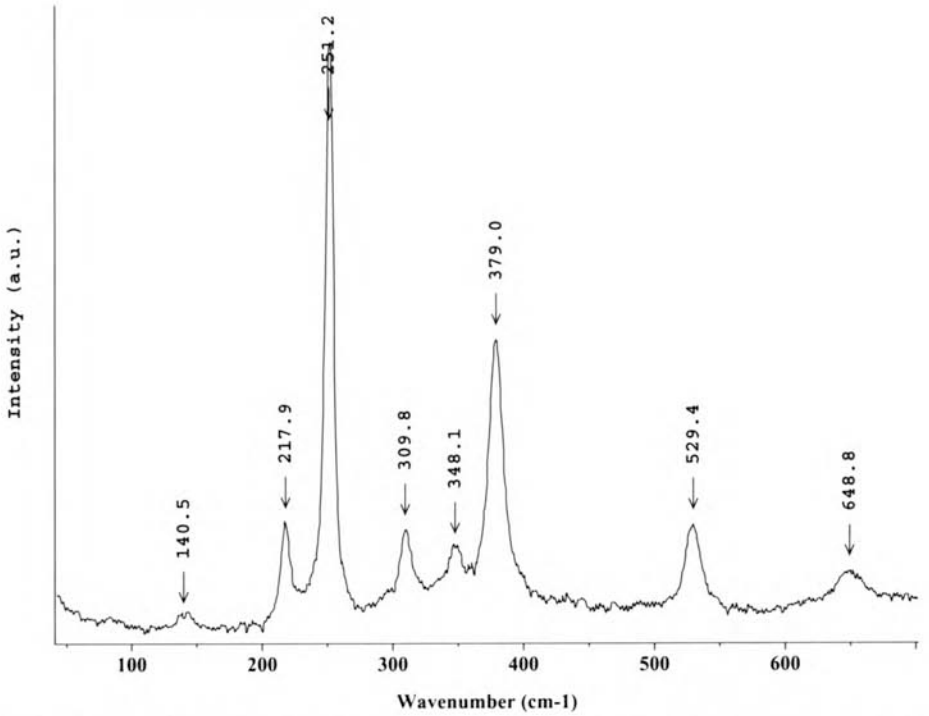

Figure 29. Raman spectrum of type (c) of oxy-hydroxide observed on the Roman ingot: (EBGU09)

Type (c) presents the bands of lepidocrocite previously quoted together with a characteristic band of maghemite at 348 cm^{-1}. The co-presence of these two species can be explained by considering the scheme proposed by Taylor and Schwertmann[108] where lepidocrocite can be transformed into maghemite by "dehydroxylation" (both being γ forms)[109]. Taylor[106,107] indicated that the presence of chlorides can be revealed by the identification of lepidocrocite on altered iron materials coming from a maritime environment. The band at 310 cm^{-1} is present in most spectra of type (c); the explanation the closest to the current data of the literature[51,52] is that this band would correspond to the anion $FeCl^{4-}$, in particular to the deformation mode of the tetrahedron $FeCl_4$. It is unknown at the moment if in our spectra the 310 cm^{-1} band represents $FeCl^{4-}$ (1) in a solute environment (intergranular or microinclusions), or (2) stabilized on

or in a mineral phase. On the other hand, Salyulev *et al.*[114] attribute for the tetrahedral anion $FeCl^{4-}$ the following Raman bands which, regrettably, do not correspond to those quoted by Boucherit *et al.*, 1991, 1992): ν_1 (A_1) = 331-344 cm^{-1}, ν_2 (E) = 115-119 cm^{-1}, ν_3 (F_2) = 374-416 cm^{-1} and ν_4 (F_2) = 131-159 cm^{-1}. Other bands of generally weak intensity, but reproducible, are visible at 138-140 and 218 cm^{-1}; these were not able to be attributed to any of the known alteration products of iron. The same type of spectrum (type (c)) was also observed on the iron medal P5. It is thus a question of determining if this type of spectrum constitutes, or not, a proof of the presence of chlorides on the object

The bands at 529 and 649 cm^{-1} have not yet been attributed to any of the known iron oxyhydroxides (the 649 band is too low to fit the wavenumber of magnetite at ~670 cm^{-1}).

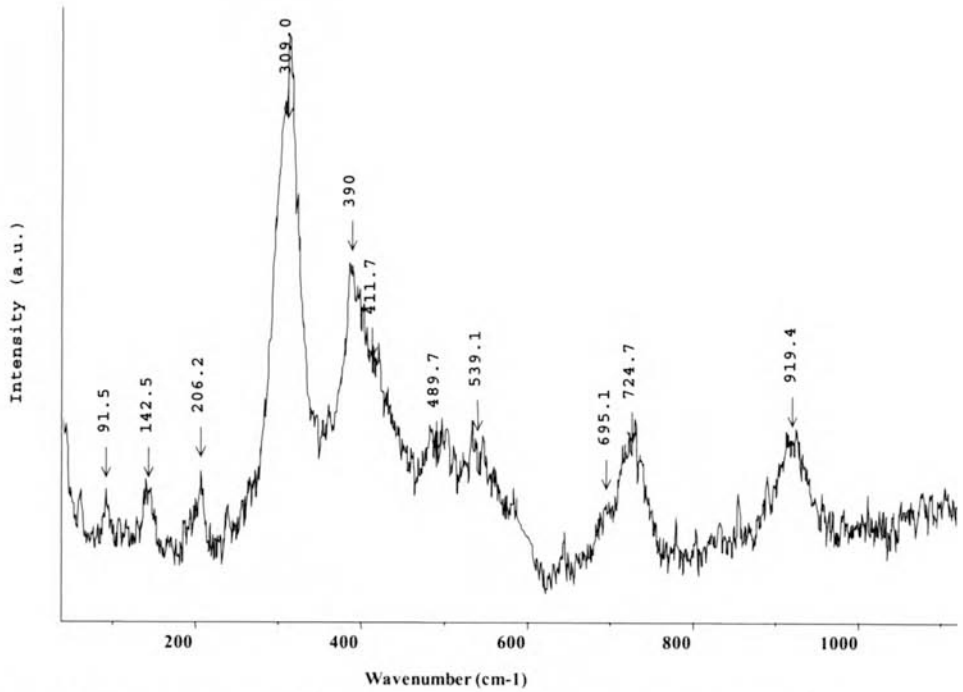

Figure 30. Raman spectrum of type (d) of oxy-hydroxide observed on the Roman ingot: (EEGU08)

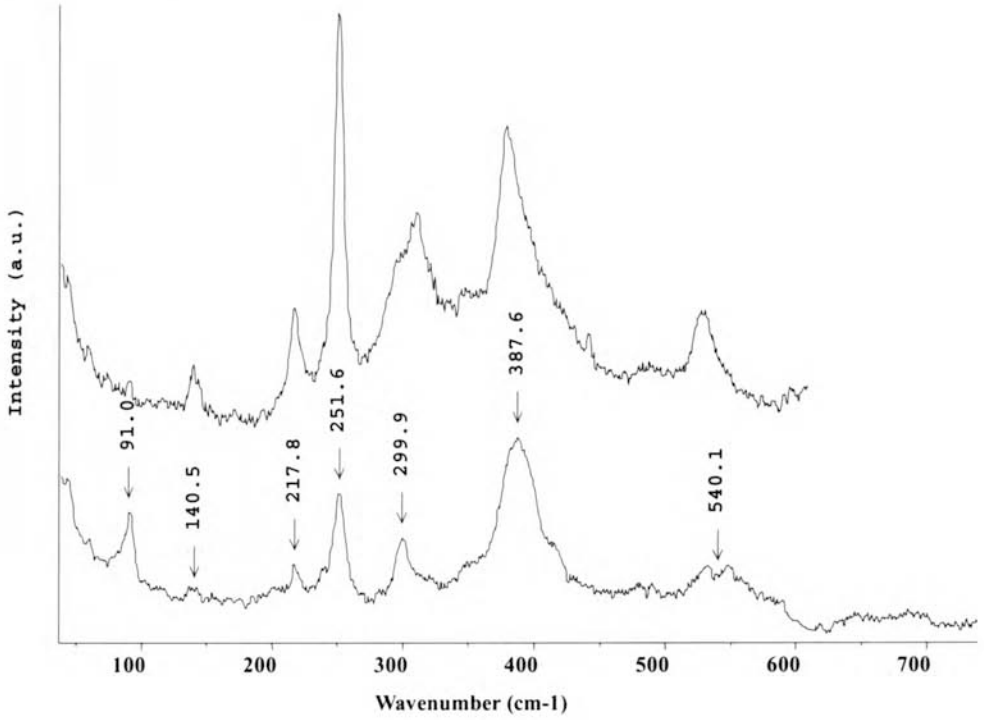

Figure 31. Raman spectra of type (e) of oxy-hydroxide observed on the Roman ingot: (ECGU02, EEGU09)

Type (d) is a mixture of akaganeite, $FeCl_4^-$ and goethite. The identification of akaganeite is based on the presence of bands at 722 and 920 cm^{-1} which always appear together and do not correspond to any other kind of iron oxy-hydroxide[45]. The band at ~ 415 cm^{-1} also corresponds, according to Boucherit *et al.*[52] to akaganeite. The goethite is identified by the bands of type (b). The co-presence of akaganeite and goethite in the Raman spectra is not surprising because, according to Cornell and Giovanoli[115], the alkaline environment would strongly favour the transformation of akaganeite into goethite and/or hematite. Other bands, less reproducible, are observed at 140 and 205 cm^{-1}; they are of very weak intensity and have not been attributed to any known alteration product of iron. The spectrum of type (d) has also been observed on the iron medal P5 except for the bands of akaganeite at 722 and 920 cm^{-1}.

Type (e) is the most complex because it seems to correspond to mixtures of four sorts of alteration: goethite (e.g. bands at 91 and 390 cm^{-1}), lepidocrocite (e.g. band at 250 cm^{-1}), maghemite (band at 349 cm^{-1}) and $FeCl_4^-$ (band at 310 cm^{-1}).

At all three stages t_0, t_1 and t_2 of the dechlorination one observes the spectrum of type (d), which is mainly characteristic of akaganeite (+ chloride). One also observes at stage t_2 lepidocrocite which thus did not disappear from this zone at the end of two dechlorinations. The band at 310 cm^{-1} is observed at the all stages of the dechlorination. If this band corresponds to a chlorine anion of type "$FeCl_4^-$ ", then iron chlorides are present in the three stages of the analysis on the surface of the ingot. Akaganeite, which is often stabilized by chlorine ions, is also found in all three stages. It is generally admitted that akaganeite is mainly observed on iron objects coming from a maritime environment[116], and that the stability of this mineral depends on the presence of chlorine ions (Cl^-) in a small quantity in its crystalline structure $\{\beta\text{-}FeO(OH)_{1-x}Cl_x\}$[117]. The presence of these chlorine ions presents a precarious, if not critical, state for the conservation of iron materials.

RM thus allowed the identification of the principal mineral species already observed by other techniques on iron objects coming from a maritime environment (goethite, lepidocrocite and akaganeite[117]); the method of dechlorination by hydrogen plasma of iron metals is a interesting new procedure but which still needs to be perfected. Reference Raman spectra of crystalline iron chlorides are still lacking in the literature and require a longer complex investigation because of the weak thermodynamical stability of these products. Furthermore, since the technique of reduction of chlorides by hydrogen plasma is based on the principle of the migration of chlorides[112] from the inside of the iron material towards the outside (layer of corrosion), then it would seem important to follow the process of migration of chlorides in three dimensions, which obviously requires obviously the semi-destructive sectioning of the object.

4.6. PRODUCTS OF ALTERATION OF OTHER METALS (AL, NI, SN)

Many other metallic objects have been studied with the same purpose of determining the capabilities of RM for the identification of the corrosion products of these types of metals. The different objects are mainly aluminium and nickel coins. The results on this type of object were not so clear compared to the metals described above, for different reasons. Aluminium forms an oxide

layer of probable composition $\{Al_2O_3\}$ that seems to be amorphous until 450°C, and from which a Raman spectrum is not normally obtained, since the size of its crystals is too small, even "unicellular" according to Scully[74]. A spectrum of rather weak intensity was however obtained on the aluminium coin (ref. G471). A band (260 cm^{-1}) of rather weak intensity and masked by a strong fluorescence was obtained. This spectrum does not compare with any known Raman spectrum of $\{Al_2O_3\}$[118].

Concerning the studied nickel coin (ref. G474), no Raman results have been achieved. Abourazzouk[119] described the Raman spectra of different oxides, hydroxides and halides of nickel such as $\{NiO\}$, $\{Ni_2O_3\}$, $\{\beta NiOOH\}$, $\{\gamma NiOOH\}$, $\{\alpha Ni(OH)_2\}$, $\{\beta Ni(OH)_2\}$, $\{NiCl_2\}$, etc. None of these products were detected on the studied coin. The very recent manufacture of this coin (1960) and the very weak aggressive surrounding alteration conditions make it likely that no significant layer of corrosion formed since the manufacture of the coin. Subsequent studies are planned to make accelerated corrosion tests on these two types of metals in order to try to identify the different possible alteration products.

No trace of alteration products of tin was discovered in any of the studied objects. Tin enters in the composition of bronzes; it was consequently conceivable to expect some trace of alteration of this component in close relation with the alterations of the copper, especially since Robbiola[81] observed by SEM/EDS a larger concentration of tin in the external layers of the altered bronze objects than in the middle of the alloy itself. A future more detailed study of the alteration of bronzes by RM would require the acquisition of Raman reference spectra of products such as, for example: romarchite $\{SnO\}$, abhurite $\{Sn_3OCl_2(OH)_2\}$, hydroromarchite $\{Sn_3O_2(OH)_2\}$ and herzenbergite $\{SnS\}$.

5. CONCLUSIONS

There exists a Greek sentence which refers to "patina" as "the flower of brass". This beautiful metonymy well symbolizes the complexity for metal of the problem with the term "patina" on archaeological or artistic objects. In the definition of the term "restoration", given by the Encyclopædia Universalis[65], one finds: "the conservation and/or the restoration of metals requires the elimination of the alteration products and the choice that one makes then, between the "patina" (agent of corrosion) which one removes and the "noble patina" which one keeps, is very interesting". Even if one does not adhere to the term of "noble patina" which was probably intended to mean here "passive", the definition given above described perfectly the role which RM can, and should, play in the archaeology of metals. Can it be pretended that there exists a "good" and a "bad" "patina"? Or is it simpler to abolish this term from the scientific language and reserve it for the artistic vocabulary. This study on the alteration products of metals evaluated the overall capacity of the RM analytical method, which is still rapidly expanding in terms of its ever-increasing applications, and applied it to the identification and characterisation of the corrosion products of archaeological materials.

The results turned out to be largely convincing for the future of this method in the precise domain of "archaeometry of metals". The identification of simple or passive alteration phases found as much interest as the identification of more complex or active phases. In the first case the layer of alteration should not be removed because of its natural passive role, i.e. it protects the object from further corrosion, whereas in the second case the alteration should be eliminated and neutralized as quickly as possible with the aim of protecting the object from a complete and definitive mineralised transformation (i.e. destruction).

Copper sulphates identified in this chapter under the form of langite and antlerite are a good example of passive alteration products, while iron and copper chlorides are good examples of active products to be fought as soon as they are detected. The examples are numerous and our purpose is not to cite them all, but rather to encourage the development of RM analysis prior to the restoration, or even on the site of first access to the altered objects. On this point it is relevant to note that metal corrosion phases can be analysed *in situ* under

water[64] in shallow seas/lakes or inside a conservation bath. Further exploitation of RM will probably allow a reduction in the difference between the number of metal materials discovered every year in France and the number of exploited and treated materials (less than half according to Robbiola[81]).

This study is far from being finished; an obvious extension would be to organic alteration products (e.g. acetates, formates or oxalates of copper or lead). Nevertheless this project is certainly a further step in the partial realization of the thought of Louis Pasteur (1865): "the possible and desirable alliance of science and art".

6. REFERENCES

1 SMITH, D. C. and EDWARDS, H. G. M. (1998). A wavenumber-searchable tabular indexed catalogue for "Archaeoraman©": Raman spectra of geomaterials and biomaterials of interest in Archaeology (sensu lato), in *ICORS Capetown' 98*, ed. A.M. Heyns, John Wiley, Chichester, 510-511.

2 SMITH, D.C., (1999): Letting loose a laser: MRM (Mobile Raman Microscopy) for Archæometry and Ethnomineralogy in the next millennium. *Invited FEATURE article, Mineral. Soc. Bulletin, December 1999*, Mineral. Soc. Great Britain, 3-8.

3 SMITH, D.C. (2002): ARCHAEORAMAN and Mobile Raman Microscopy (MRM): from pigments in aerial wall-paintings to gemstones in submarine archaeometry. Congress *Georaman-2002*, Acta Universitatis Carolinae, Geologica, Praha, v46, n°1, 84-86.

4 DELHAYE, M., GUINEAU, B.,VEZIN, J. AND COUPRY, C. (1985). La microsonde Raman au secours des oeuvres d'art, *Mesures* 11, Paris, 119-124.

5 BELL, I. M., CLARK, R. J. H. and GIBBS, P. J., (1997), Raman spectroscopic library of natural and synthetic pigments (pre- ~1850 AD), *Spectrochimica acta*, 53, part A, 2159-2179.

6 RULL-PEREZ, F., EDWARDS, H.G.M., RIVAS, A. and DRUMMOND, L. (1999), Fourier Transform Raman Spectroscopic characterization of pigments in the Mediaeval frescoes at Convento de la Peregrina, Sahagun, Léon, Spain. Part 1 – Preliminary Study. *Journ. Raman Spectroscopy* 30, 301-305.

7 WITHNALL, R., (1999), *In situ identification of pigments, Manuscripts and prints using Raman Microscopy*, GEORAMAN'99, Valladolid, SPAIN, University of Valladolid, 15-16.

8 SMITH, D.C., (2000): Pigments rouges et bleus sur cinq oeuvres d'Amérique: Analyse non-destructive par MRM (Microscopie Raman Mobile). *Techne 11*, Louvre , Paris, 69-83.

9 VANDENABEELE, P., MOENS, L., EDWARDS, H.G.M. and DAMS, R., 2000, Raman spectroscopic database of azo-pigments and application to modern art studies, *J. of Raman Spectrosc.*, 31, n°6, 509-517.

[10] BURGIO L, CLARK R.J.H. and FIRTH S. (2001), Raman spectroscopy as a means for the identification of plattnerite (PbO2), of lead pigments and of their degradation products, *Analyst*, 126, no 2, pp. 222–227.

BURGIO L and CLARK R.J.H. (2001), Library of FT-Raman spectra of pigments, minerals, pigment media and varnishes, and supplement to existing library of Raman spectra of pigments with visible excitation, *Spectrochimica Acta Part A*, 57, 1491–1521.

[11] RULL-PEREZ, F., (2001), Applications of IR and Raman Spectroscopy to the study of Medieval Pigments. Chapter 21, p. 835-862 in: *A Handbook on Raman Spectroscopy*, I.LEWIS and H.G.M.EDWARDS (eds), Marcel Dekker Inc., New York.

[12] EDWARDS, H.G.M., BARRY, B.W., WILLIAMS, A.C. and RULL, F. (1996a). The Iceman: an FT-Raman spectroscopic study of 5200-year-old human skin, GEORAMAN-96, *Terra Abstracts*, Suppl. N°. 2 of *Terra Nova*, 8, 1.

[13] EDWARDS, H.G.M., DAFFNER, L.A., FALK, M.J., FARWELL, D.W., HERON, C. and QUYE, A. (1996b). FT-Raman spectroscopic analyses of ancient resins of archaeological significance, GEORAMAN-96, *Terra Abstracts*, Suppl. N°. 2 of *Terra Nova*, 8, 1.

[14] EDWARDS, H.G.M., FALK, M.J., FARWELL, D.W. and JANAWAY (1996c). FT-Raman spectroscopic studies of linen samples from archaeological burial sites, GEORAMAN-96, *Terra Abstracts*, Suppl. N°. 2 of *Terra Nova*, 8, 2.

[15] BRODY, R. H., EDWARDS, H.G.M., FARWELL, D.W., O'CONNOR, S. and POLLARD, A. M. (1998). Real or fake: FT-Raman study of ivories, in: *ICORS Capetown' 98*, ed. A.M. Heyns, John Wiley, Chichester, 522-523.

[16] DELE-DUBOIS M.L., DHAMELINCOURT P. and SCHUBNEL H.J., (1981a,b), Etude par spectrométrie Raman d'inclusions dans les diamants, saphirs et émeraudes. *Revue de Gemmologie, Assoc. Franç. Gemmologie*, Paris, 63, 11-14, and 64, 13-14.

[17] PINET, M., SMITH, D. C. and LASNIER, B., (1992), Utilité de la microsonde Raman pour l'identification non-destructive des gemmes, avec une sélection représentative de leurs spectres Raman. Chap. II, p. 11-61 dans "*La Microsonde Raman en Gemmologie, Revue de Gemmologie*", n° spécial hors série, 61 p.

[18] SMITH, D.C. and ROBIN, S. (1997): Early-Roman Empire intaglios from "rescue excavations" in Paris: an application of the Raman Microprobe to the non-destructive characterisation of archaeological objets. *J. Raman Spectrosc.* 28, n° 2 and 3, 189-193.

[19] KIEFERT, L., HÄNNI, H.A. and OSTERTAG T., (2001a) Raman Spectroscopic Applications to Gemmology. Chapter 11, 469 in, *A Handbook on Raman Spectroscopy*, I. Lewis and H.G.M. Edwards, eds Marcel Dekker Inc., New York, 2001.

[20] SMITH, D.C. (2004a): Jewellry and precious stones. In: *Raman Spectrometry in Archaeology and Art History*, eds: Edwards, H.G.M and Chalmers J., The Royal Society of Chemistry, London (in press).

[21] SMITH, D. C. and GENDRON, F. (1997). Archaeometric Application of the Raman Microprobe to the Non-Destructive Identification of Two Pre-Columbian Ceremonial Polished "Greenstone" Axe Heads from Mesoamerica, *J. of Raman Spectrosc.*, 28, 731 - 738.

[22] SMITH D.C. and BOUCHARD, M., Petroraman, *Archéométrie, Dossiers de l'Archéologie*, 2000a, 253, May 2000, 54.

[23] SMITH, D.C. and CARABATOS-NEDELEC, C., (2001): Raman Spectroscopy Applied to Crystals: Phenomena and Principles, Concepts and Conventions. Chapter 9, 349-422 in: *A Handbook on Raman Spectroscopy*, I.LEWIS and H.G.M.EDWARDS (eds), Marcel Dekker Inc., New York.

[24] NASDALA, L., SMITH, D.C., KAINDL, R. and ZIEMANN, M.A., in "*EMU Notes in Mineralogy, EMU School on Spectroscopic Methods in Mineralogy*", eds. A. Beran and E. Libowitzky, 2004, (in press).

[25] SMITH, D.C. (2004b): Mesoamerican jade. In: *Raman Spectrometry in Archaeology and Art History,* eds: Edwards, H.G.M and Chalmers J., The Royal Society of Chemistry, London (in press).

[26] CLARK, R. J. H., CURRI, L., HENSHAW, G. S. and LAGANARA, C., Characterization of brown-black and blue pigments in glazed pottery fragments from Castel Fiorentino (Foggia, Italy) by Raman microscopy, X-ray powder diffractometry and X-ray photoelectron spectroscopy *J. Raman Spectrosc.* 1997, 28, 105.

[27] FRY, R.L., FROST, R.L., TURNER J. and HALLAM, D. (1998). Analysis of ceramics from the wreck of the "Pandora" using Raman and FTIR spectroscopy, in: *ICORS Capetown' 98*, ed. A.M. Heyns, John Wiley, Chichester, 546-547.

[28] LIEM, N.Q., SAGON, G., QUANG, V.X., TAN, H.V. and COLOMBAN, P., Raman study of the microstructure, composition and processing of ancient Vietnamese (proto)porcelains and celadons (13-16th centuries), *J. of Raman Spectrosc.*, 2000, 31, 933.

[29] COLOMBAN, P. and TREPPOZ, F., (2001), Identification and differentiation of ancient and modern European porcelains by Raman macro- and micro-spectroscopy, *J. Raman Spectrosc.*, 32, 93-102.

[30] COLOMBAN, P., SAGON, G. and FAUREL, X., Differentiation of Antique Ceramics from the Raman Spectra of their Coloured Glazes and Paintings, *J. of Raman Spectrosc.* 32, 2001, pp. 351-60.

[31] COUPRY, C., SAGON, G. and LAUTIE, A., (1993), *Contribution par Spectrométrie Raman à la connaissance des vitraux.*, Conservation commune d'un patrimoine commun. 1èr colloque du Programme franco-allemand de recherche pour la conservation des monuments historiques, Karlsruhe, 246-249

[32] MACQUET, C., (1994), Contribution à l'étude des surfaces vitreuses anciennes; application à l'amélioration des techniques de conservation, *Thèse de doctorat*, Poitiers, 198 p.

[33] EDWARDS, H.G.M. and J. F. K. TAIT, FT-Raman spectroscopic study of decorated stained glass, *Applied spectroscopy*, 1998, 52, 5, 679.

[34] SMITH, D. C., BOUCHARD, M. A. and LORBLANCHET, M., (1999a), An Initial Raman Microscopic Investigation of Prehistoric Rock Art in Caves of the Quercy District, S.W.France, *J. of Raman Spectrosc.*, 30, 347-354.

SMITH D.C., CARABATOS-NEDELEC C. and BOUCHARD M., (1999b): Vitroraman: establishing a database on the Raman spectra of pigments on and in stained glass. *Georaman'99, Abstracts, Special Pub.* Valladolid Univ. Press, Spain, 36-37.

[35] BOUCHARD, M. and SMITH, D.C. (2001): Evaluating Raman Microscopy for the non-destructive archaeometry of corroded coins: a powerful technique the conservation studies. *Asian Chemical Letters*, 5 n° 3, 157-170.

[36] BOUCHARD, M. and SMITH, D.C. (2002): Archaeological and Experimental Stained Glass: a Non-Destructive Raman Microscopic (RM) Study. "ART 2002", *7th International Conference on Non-destructive Testing and Microanalysis for the Diagnostics and Conservation of the Cultural and Environmental heritage*, University of Antwerp, June 2002, Abstract vol., p. 152.

[37] WANG. C., LU, B., ZUO, J., SUZUKI, M. and CHASE, W.T., (1995), Structural and elemental analysis of the nanocrystal SnO2 in the surface of ancient Chinese black mirrors, *Nanostructured materials*, 4, 489-496.

38 MCCANN, L. I., TRENTELMAN, K., POSSLEY, T. and GOLDING, B., (1999), Corrosion of ancient chinese bronze money trees studied by Raman Microscopy, *J. of Raman Spectrosc.*, 30, 121-132.

39 BOUCHARD, M. AND SMITH, D. C., (1999), *Corroded antique and modern coins studied by Raman Microscopy*, *Georaman'99*, Valladolid/Spain, University of Valladolid, 31-32.

BOUCHARD, M. and SMITH, D. C. (1999). Metalloraman: corroded antique and modern coins studied by Raman Microscopy, *Georaman'99 abstracts*, *Special Pub.* Universidad Valladolid Press, Valladolid, 31-32.

40 BOUCHARD, M. and SMITH, D. C., (2000a), METALLORAMAN, *Archéométrie, Dossiers de l'Archéologie*, **253**, 60-61.

41 BOUCHARD, M. and SMITH, D. C., (2000b), *A mini-catalogue of metallic corrosion products studied by Raman microscopy*, CSM2, 2ème colloque franco-libanais sur la science des matériaux, Beyrouth, Lebanon, 37.

42 BOUCHARD, M. and SMITH, D. C., (2000c), New data for the application of Raman microscopy to archaeological corroded metallic objects, *ICORS'2000, Beijing*, China., 1140-1141.

43 BOUCHARD, M. and SMITH, D.C. (2003): Catalogue of 45 Reference Raman Spectra of Minerals concerning research in Art History or Archaeology, especially on corroded metals and coloured glass. Spec. Vol., Proceedings, GEORAMAN-2002 congress, Prague, 2002, *Spectrochimica Acta*, Part A, 59, 2247-2266.

44 BOUCHARD, M. and SMITH, D.C., (2004) Database of 74 Raman Spectra of Standard Minerals of relevance to metal corrosion, stained glass or Prehistoric rock art Chapter 25 In "*Raman Spectroscopy in Archaeology and Art History*", eds. H.G.M. Edwards and J.M. Chalmers, RSC, Cambridge, UK, 2004, (in press).

45 BOUCHARD, 2001, (5 décembre 2001), Évaluation des Capacités de la Microscopie Raman dans la Caractérisation Minéralogique et Physico-chimique de Matériaux Archéologiques : Métaux, Vitraux and Pigments, *thèse de Doctorat*, Muséum National d'Histoire Naturelle, Paris, pp.360.

46 FROST, R.L., MARTENS, W., KLOPROGGE, T. and WILLIAMS, P.A., Raman Spectroscopy of the basic Copper Choride Minerals Atacamite and Paratacamite: Implications for the study of Copper, Brass and Bronze Objects of Archaeological Significance, *J. of Raman Spectrosc.*, 2002a, 33, 801.

47 FROST, R.L., WILLIAMS, P.A., MARTENS, W. and KLOPROGGE, T., Raman Spectroscopy of the Polyanionic Copper (II) Minerals Buttgenbachite and Connellite: Implications for studies of Ancient Copper Objects and Bronzes, *J. of Raman Spectrosc.*, 2002b, 33, 752.

48 TRENTELMAN, K., STODULSKI, L., SCOTT, D., BACK, M., STOCK, S., STRAHAN, D., DREWS, A.R., O'NEILL, A., WEBER, W.H., CHEN, A.E. and GARRETT, S.J., The characterization of a new pale blue corrosion product found on copper alloy artefacts *Studies in Conservation,* 2002.

49 PARDESSUS-PEYROL, P., (1986), Contribution à l'étude du mécanisme de corrosion du Cupro-Nickel en milieu chlorure de sodium à 3%, *Thèse de doctorat*, Aix-marseille, Aix-marseille, 148 p.

50 DELICHERE, P., HUGOT-LE-GOFF, A. and JOIRET, S., (1987), In situ characterization of thin corrosion films on alloys by Raman spectroscopy, *Le vide, Les couches minces*, 235, 465.

[51] BOUCHERIT, N., HUGOT-LE-GOFF, A. and JOIRET, S., (1991), Raman studies of corrosion films grown on Fe and Fe-6Mo in pitting conditions, *Corrosion Science*, 32, 5-6, 497-507.

[52] BOUCHERIT, N., HUGOT-LE-GOFF, A. and JOIRET, S., (1992), In situ Raman identification of stainless steels pitting corrosion films., *Mater. Sci. Forum*, Electrochem. Methods Corros. Res., 581-7, 111-112.

[53] THIERRY, D., MASSINON, D. and HUGOT-LE-GOFF, A., (1991), In situ determination of corrosion products formed on painted galvanized steel by Raman Spectroscopy, *J. Electrochem. Soc.*, 138, 3, 879 – 880.

[54] HUGOT-LE-GOFF, A., MASSINON, D., PHILLIPS, N., (1992), In situ Raman identification of corrosion products on galvanized steel sheets, *Materials science Forum*, 617, 111-112.

[55] HUGOT-LE-GOFF, A., BERNARD, M. C. and PHILLIPS, N., (1995), Contributions of Raman spectroscopy and electrochemical impedance to the understanding of the underpaint corrosion process of zinc-coated steel sheets., *Mater. Sci. Forum*, 192-194.

[56] BERNARD, M. C., HUGOT-LE-GOFF, A. and VU-THI, B., (1993a), Electrochromic Reactions in Mn Oxides, *J. Electrochemical Soc.*, 140, 11, 3065.

[57] BERNARD, M. C., HUGOT-LE-GOFF, A. and MASSINON, D., (1993b), Underpaint corrosion of zinc caoted steel sheet studied by in situ Raman spectroscopy, *Corrosion science*, 35, 809.

[58] BERNARD, M. C., CORDOBA-DE-TORESSI, S. and HUGOT-LE-GOFF, A., (1994), Electrochromic reactions in MnO_2 Films polarized in neutral solution, *Proceedings of the symposium on Electrochromic materials II*- 94-2,

[59] BERNARD, M. C., HUGOT-LE-GOFF, A. and PHILLIPS, N., (1995a), In situ Raman study of zinc-coated steel in presence of chloride. Characterization and stability of zinc corrosion products, *Journal of Electrochemical Society*, 142, 7, 2162-2167.

[60] BERNARD, M. C., HUGOT-LE-GOFF, A. and PHILLIPS, N., (1995b), In situ Raman study of zinc-coated steel in presence of chloride. II. Mechanisms of underpaint corrosion and role of the conversion layers., *Journal of Electrochemical Society*, 142, 7, 2167-2170.

[61] SMITH, D.C. (2004c): Raman micromapping of physical and/or chemical transformations of minerals of interest in Geology or Archaeology. *Georaman-2004*, Univ. Hawaii, Honolulu, Hawaii, 6-11 June 2004, publ. SOEST 04-02 (School of Ocean and Earth Science Technology), 71.

[62] SMITH, D.C. (2004d): Raman Micro-mapping of chemical and/or physical mineral phase transformations involving jadeite, coesite, diamond or zircon in natural ultra-high pressure metamorphic environments (UHPM). *XIXth International Conference on Raman Spectroscopy*, ICORS, Gold Coast, Australia, 8-13 August 2004, Proceedings, (eds.) P.M.Fredericks, R.L.Frost and L.Rintoul, CD-ROM.

[63] SMITH D.C. and RONDEAU B, (2001): Non-destructive mineralogical analysis of precious stones in situ under thick glass by MRM (Mobile Raman Microscopy). Congress "*Archéométrie 2001*", GMPCA, La Rochelle, p. 101.

[64] SMITH, D.C. (2003): In situ mobile Subaquatic Archaeometry evaluated by non-destructive Raman Microscopy of gemstones lying under impure waters. Spec. Vol., Proceedings, GEORAMAN-2002 congress, Prague, 2002, *Spectrochimica Acta*, Part A, 59, 2353.

[65] ENCYCLOPEDIA UNIVERSALIS, (1997), CD-ROM, electronic source.

66 POURBAIX, M., (1977), Electrochemical corrosion and reduction *in Corrosion and metal artefacts- a dialogue between conservators and archaeologists and corrosion scientists*, ed. Brown, B. F., 1-16.

67 MOUREY, W., (1987), *La conservation des antiquités métalliques, de la fouille au musée*, Bonnaud, Draguignan, 127.

68 EVANS, U.R., (1928), *La corrosion des métaux*, Dunod, Paris, 323 p.

69 BERNARD, J., (1962), *Oxydation des métaux, Monographie tome II*, Gauthier-Villars ed., Paris.

70 POURBAIX, M., (1966), *Atlas of electrochemical equilibra in aqueous solution*, Pergamon-press, London, 76-79.

71 LEIDHEISER, H. J., (1971), *The corrosion of copper, tin and their alloys*, John Wiley and sons, N.Y, 411 p.

72 FUVELLE, C., (1979), *Introduction à la corrosion, formes et préventions*, Paris.

73 BERNARD, J., MICHEL, A., PHILIBERT, J. and TALBOT, J., (1984), *Métallurgie générale*, Masson ed., Paris.

74 SCULLY, J. C., (1990), *The fundamental of corroson 3rd Ed*, Pergamon Press, Oxford, 226 p.

75 PHILIBERT, J. and VIGNES, A., (1998), *Métallurgie : du minerai au matériau*, ed. Masson, paris, 1107 p.

76 SEAR, D. R., (1988), *Roman coins and their values*, London, 387 p.

77 KRAUSE, C.L., (1991), *World coins*, 17ème ed., Bruce L.R. Ed., 1936 p.

78 GADOURY, (1993), *Monnaies Françaises de 1789 à 1992*, Paris, p. 368.

79 QAFSAOUI, W., (1992), Sensibilité du cuivre pur ou faiblement allié à la corrosion par des piqûres dans des solutions tampons contenant des ions chlorures, sulfates ou nitrates, *Thèse de doctorat*, Univ. Toulouse.

80 MEYER-ROUDET, H., (1999), *A la recherche du métal perdu, les nouvelles technologies dans la restauration des métaux archéologiques*, Catalogue d'exposition, M.A.D.V.O. Errance, Paris, 192.

81 ROBBIOLA, L., (1990), Caractérisation de l'altération de bronzes archéologiques enfouis à partir d'un corpus d'objets de l'âge du bronze: mécanisme de corrosion, *Thèse de doctorat*, Jussieu, Paris VI, Paris, 121 Ref.

82 JAMBOR, J., DUTRIZAC, J. and ROBERTS, A., (1996), Clinoatacamite, a new polymorph of Cu2(OH)3Cl, and its relation to paratacamite and 'anarakite', *the Canadian mineralogist*, 34, 61-65.

83 MARTENS W., FROST R.L. and WILLIAMS P.A., (2003), Raman and infrared spectroscopic study of the basic copper chloride minerals: implications for the study of the copper and brass corrosion and "bronze disease", *Neues Jahrbuch für Mineralogie. Abhandlungen,* **178**, no 2, pp. 197 – 215.

84 GUINEAU, (1987), L'étude des pigments par les moyens de la Microspéctrometrie Raman, in "*Datation-Caractérisation des peintures pariétales et murales (PACT-17)*", ed. F. Delamare, T. Hackens and B. Helly, European University Centre for Cultural Heritage, Ravello, 1987, chap. II.2.2, p. 259-294.

85 RIBBE, P. H. AND ERIKSSON, S. C., (Janvier-Fevrier 1991), *FM-TGMS-MSA Symposium on Azurite and other copper carbonates*, Blacksburg, Virginia, USA, The Mineralogical Record, 22, 65-69.

86 CHAPMAN and HALL (1998), MinSource, CD-ROM, electronic source.

87 SCHMIDT, M. and LUTZ, H. D., (1993), Hydrogen Bonding in basic Copper Salts: a Spectroscopic study of Malachite $Cu_2(OH)_2CO_3$, and Brochantite, $Cu_4(OH)_6SO_4$, *Phys. Chem. Minerals*, 20, 27-32.

88 ADDA, Y., DUPOUY, J. M., PHILIBERT, J. and QUERE, Y., (1982), Corrosion in Elements de Métallurgie physique, *Tome 6*, ed CEA, Paris, 1815-1875.

89 MACHEFERT, J. M., (1990), Contribution des méthodes spectroscopiques d'analyse à l'étude de l'oxydation du cuivre ofhc, *Thèse de doctorat*, Université de Rouen, Rouen.

90 CARABATOS, C., (1970), Lattice vibrations of Cu_2O at the long Wave limit, *Phys. stat. sol.*, 37, 773.

91 CARABATOS, C., (1971), Etude de la dynamique du réseau de CuCl, SiC, Cu_2O, Ag_2O et Cu-Zn, *Thèse de doctorat*, Université Louis Pasteur de Strasbourg, Strasbourg, 139 p.

92 XU, J., JI, W., WANG, X.B. and SHU, H., (1998), Temperature dependence of the Raman scattering spectra of Zn/ZnO nanoparticles, *J. of Raman Spectrosc.*, 29, 613-615.

XU, J., JI, W., SHEN, Z. H. and LI, W.S, (1999), Raman Spectra of CuO nanocrystals, *J. of Raman Spectrosc.*, 30, 413-415.

93 REYDELLET, J., (1970), *Thèse de doctorat*, Univ. Paris.

94 KUGEL, G., CARABATOS, C. and KRESS, W., (1983), *Lattice dynamics of cuprite (Cu_2O)*, AB initio calculation of phonon spectra, Ed. J.T. Devreese, Planum Pub. Corp., 101-.

95 LE-GAL-LA-SALLE-MOLLIN, A., (1991), Corrosion, passivation et protection du cuivre en solution aqueuse, *Thèse de doctorat*, Jussieu, Paris VI, Paris.

96 SCOTT, D. A., (2000), A review of copper chloride and related salts in bronze corrosion and as painting pigments, *Studies in conservation*, 45, 39-53.

97 DAMEN, T. C., PORTO, S. P. S. and TELL, B., (1966), Raman effect in zinc oxide, *Phys. Rev.*, 142, 2, 570.

98 PHILLIP, N., (1993), Corrosion sous peintures de tôles d'acier éléctrozinguées : identification des produits de corrosion du zinc par spectrométrie Raman et caractérisation du comportement électrochimique par la méthode d'impédance, *Thèse de doctorat*, Jussieu, Paris VI, Paris, 210 p.

99 SANGAMESHWAR, S.R. and BARNES, H.L., (1983), Supergene processes in zinc-lead-silver sulphide ores in carbonates, *Ecionomic Geology*, 75, 1379-1397.

100 TLILI, A. and SMITH, D.C. (2004) Raman spectroscopic study of synthetic Na-Mg-Al-Si trioctahedral micas compared with their Ge- and Ga-equivalents. In "*Georaman and Archaeoraman*", Universidad Valladolid, eds. F.RULL, D.C.SMITH & H.G.M.EDWARDS, (this book).

101 PREVOT, B. and CARABATOS, C., (1971), Dynamique du réseau de l'argentite (Ag_2O), *Le journal de Physique*, 32, 543-546.

102 PASCAL, P., (1963), Nouveau traité de Chimie Minérale, *Tome VIII*, Masson and Cie, Paris.

103 BROOKER, M. H., SUNDER, S. and TAYLOR, P., (1983), Infrared and Raman spectra and X-ray diffraction studies of solid lead (II) carbonates., *Can. J. Chem.*, 61, 494.

104 MASON, BRIAN, (1943), Mineralogical aspects of the system $FeO-Fe_2O_3-MnO-Mn_2O_3$, *Geol. Fören. Förh.*, 65, 97-180.

105 LINDSLEY, D. H., (1976), The crystal chemistry and structure of oxide minerals as exemplefield by Fe-Ti oxides *in Review in Mineralogy, Oxide Minerals*, 3, ed. Rumble, D., Washington, 1-25.

[106] TAYLOR, R. M., (1984a), Influence of chloride on the formation of iron oxides from FeII chloride. I. Effect of (Cl)/(Fe) on the formation of magnetite., *Clays and clay minerals*, 32, 3, 167-174.

[107] TAYLOR, R. M., (1984b), Influence of chloride on the formation of iron oxides from FeII chloride. II. Effect of (Cl) on the formation of lepidocrocite and its crystallinity., *Clays and clay minerals*, 32, 3, 175-180.

[108] TAYLOR, R. M. and SCHWERTMANN, U., (1974), Maghemite in soils and its origin. II. Maghemite sunthetis at ambiant temperature and pH, *Clay Miner.*, 10, 299-310.

[109] DE-FARIA, D. L. A., SILVA, S. V. and OLIVEIRA, M. T. D., (1997), Raman Microscopy of some Iron Oxides and hydroxides, *J. of Raman Spectrosc.*, 28, 873-878.

[110] BOUCHERIT, N., (1990), Application de la spectroscopie Raman à l'étude de la corrosion électrochimique du fer et des aciers inoxydables., *Thèse de doctorat*, Univ. Paris VI, Paris, 103 Ref.

[111] BOUCHARD, M., (1998), *Etude des pigments de grottes ornées du Paléolithique par Microscopie Raman*, mémoire de DEA, IPH, Muséum national d'Histoire Naturelle, Paris, 66 p.

[112] ARNOULD-PERNOT, P., (1994), Traitement de déchloruration des objets archéologiques ferreux par plasma d'hydrogène., *Thèse de doctorat*, Ecole des mines de Nancy, Institut National Polytechnique de Lorraine, Nancy, 157 p.

[113] ARC'ANTIQUE, (mai 2000), *Note d'information PCR fers chlorurés.* Unpub. report.

[114] SALYULEV, A. B., VOVKOTRUB, E. G. and STREKALOVSKY, V. N., (2000), Synthesis and Raman spectra of complex compounds $FeCl_3$ with alkali and alkali-earth metal chlorides, *ICORS, Beijing/China*, Wiley, 710-711.

[115] CORNELL, R. M. and GIOVANOLI, R., (1990), Transformation of Akaganéite into Goethite and hématite in alkaline média, *Clays and Clay Minerals*, 38, 5, 469-476.

[116] GILBERG, M.R, SEELEY, M.J., (1981), The identity of compounds containing chloride ions in marine ion corrosion products, a critical review, *Studies in Conservation*, **26**, 50-56.

[117] ARNOULD-PERNOT, P., FORRIERES, C., MICHEL, H. and WEBER, B., (1994), Optimisation d'un traitement de déchloruration d'objets ferreux par plasma d'hydrogène, *Studies in Conservation*, 39, 232-240.

[118] ZUO, C. and JAGODZINSKI, W., (2000), *Raman spectroscopic studies of aluminium oxides*, ICORS'2000, Beijing, China, Wiley and Sons, 614-615.

[119] ABOURAZZOUK, D., (1996), Etude par Spectrométrie Raman de la corrosion des alliages dentaires à base de Ni-Cr et influence des éléments qui composent ces alliages, *Thèse de doctorat*, Jussieu, Paris VI, Paris, 132 p.

[120] PONTING, M. and SEGAL, I., (1998), Inductively coupled Plama-atomic emission spectroscopy of roman military copper-alloy artefacts from the excavation at Masada, Israel., *Archaeometry*, 40, 1, 109-122.

[121] G. DI LONARDO, C. MARTINI, F. OSPITALI, G. POLI, D. PRANDSTRALLER AND F. TULLINI "Raman and IR micro-spectroscopy for the study of corrosion products on archaeological bronze objects", in *Proceedings of Art 2002, 7th International Conference on "Non-destructive Testing and Microanalysis for the Diagnostics and Conservation of the Cultural and Environmental Heritage"*, 2-6 June 2002, Antwerp, Belgium, Ed. by R. Van Grieken, K. Janssens, L. Van't dack and G. Meersman, p. 1-7.

[122] F. OSPITALI, T. SABETTA, F. TULLINI, M.C. NANNETTI and G. DI LONARDO, "The role of Raman micro-spectroscopy for the study of black gloss coating in Roman pottery", *Journal of Raman Spectroscopy* (accepted July 2004).